Response to Reviewer #1

General Remarks:

This paper presents an experimental study of SOA formation from dilute exhaust from two gasoline powered vehicle (Euro I and Euro 4) operated on Euro 3 gasoline. The vehicles were tested at idle. A total of five experiments were performed. The dilute exhaust was photo-oxidized in a smog chamber and substantial SOA was formed (exceeding the primary organic aerosol emissions). The paper calculated effective yields (~3 to 17%) and evaluated SOA mass closure (50-90% of SOA could be explained with measured precursors).

The basic experiments are quite similar to other recent papers on SOA formation from gasoline vehicle exhaust. The results also fall within the range of results from hose previous paper. It does expand the dataset on gasoline vehicle exhaust. The paper emphasizes the Chinese context as novel ("first" experiments performed in China). Not clear how important it is to perform these experiments in China, since China follows European emissions and fuel standards. The very small number of vehicles (2) and limited tests (5) all performed at idle (a very limited operating mode) makes it hard to draw much insight into SOA formation from in use vehicle operations. Therefore, the paper contributes little new knowledge.

The paper is well organized and the experiments were performed with high quality instrumentation.

Reply: As shown in the "Introduction" section in the manuscript, though China follows European fuel standards, gasoline fuel in China has relatively higher mass content of alkenes and aromatic hydrocarbons than that in US (Schauer et al., 2002; Zhang et al., 2013). The emission factors of $PM_{2.5}$, organic carbon (OC), element carbon (EC), NO_x, SO_2, NH_3 and non-methane hydrocarbons (NMHCs) for on-road vehicles in China were quite different from those in other countries (Liu et al., 2014; Y. L. Zhang et al., 2015). Given that the possession of LDGVs in China was 98.8 million in 2012 and increased at a rate of approximately 20% per year since 2005 (NBSC, 2013), and that gasoline cars are considered "cleaner" than diesel ones in

China, it is urgent to investigate the SOA formation from LDGVs in China in order that we can assess both primary and secondary contribution from gasoline vehicles and help formulate future vehicle emission control strategies taking the secondary formation into consideration. As diesel vehicles are considered dirtier, in many China's large cities they are not allowed to enter the core urban areas as a measure to lower urban pollution. Our study suggests gasoline cars are not so innocent and clean if considering secondary contributions. This is particularly important since SOA contributed substantially to $PM_{2.5}$ and ozone pollution is becoming more and more serious in China's megacities. We know that it would be much better to conduct more chamber simulations with more cars. However, it is not so easy to do this in a large chamber with regard to the costs and managements. We would find resources to do more based on this study. We have added some words to mention this quite limited number of experiments in the revised manuscript (lines 359-362):

"It is important to note that the reported data are only based on five chamber experiments with two LDGVs under idling conditions. More tests are needed to assess SOA formation from gasoline vehicle exhausts in China."

Specific comments:

Q1- The exhaust was transferred through Teflon transfer line and a GAST rotary vane pump (not clear if the system was heated). This set up likely caused substantial losses of both PM and VOCs before the chamber (we never use Teflon lines for PM sampling). Were these losses characterized? If not, it makes the results largely qualitative and every presentation of effective yield or mass closure needs to be qualified with this substantial uncertainty. Presumably there is less issues with the composition information (Figure 8).

Reply: A flow rate of as high as 20 L min^{-1} and a transfer line of as short as 5 m were used to provide residence time within seconds, and thus reduce the losses of particles and VOCs in the transfer lines. Furthermore, before being introduced into the reactor, gasoline vehicle exhausts were generally pumped through the transfer lines for half an hour to saturate the transfer lines with particles and VOCs while warming the

catalytic converter. Losses of particles and VOCs in the introduction lines were determined by comparing the concentrations of total particle number and VOCs in the directly emitted exhausts and the ones after passing through the transfer lines. As shown in Figure 1, the distributions of particle number in the directly emitted exhausts and the ones after passing through the transfer lines were similar. The loss of total particle number was estimated to be less than 3%. The penetration efficiency of particles in the transfer line was also estimated by a laminar diffusional deposition model (Gormley and Kennedy, 1949). For particles with diameters larger than 10 nm, the penetration efficiency was higher than 95%, indicating minor losses of particles in the transfer line. The losses of VOCs in the transfer line were estimated to be less than 5%, which might lead to a small underestimation of SOA production.

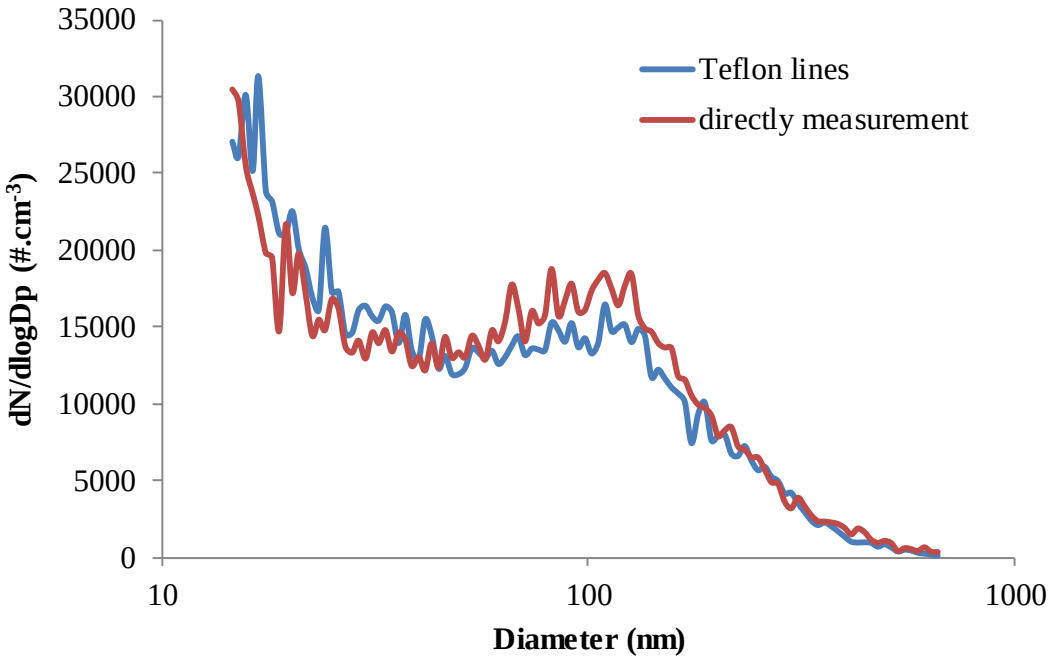

Figure 1. Particle number distributions of the directly emitted exhausts and the ones after passing through the transfer lines.

The following text has been added to the revised manuscript.

"During the introduction of exhausts, particles and VOCs might deposit to the surface of the transfer lines. Therefore, a flow rate of as high as 20 L min^{-1} and a transfer line of as short as 5 m were used to provide residence time within seconds, and thus reduce the losses of particles and VOCs in the transfer lines. Furthermore, before

being introduced into the reactor, exhausts were generally pumped through the transfer lines for half an hour to saturate the transfer lines with particles and VOCs while warming the catalytic converter. Losses of particles and VOCs in the introduction lines were determined by comparing the concentrations of total particle number and VOCs in the directly emitted exhausts with the ones after passing through the transfer lines. The loss of total particle number was estimated to be less than 3%. The penetration efficiency of particles due to diffusion in a cylindrical tube, $\eta(dp)$, can be also estimated by a laminar diffusional deposition model (Gormley and Kennedy, 1949). For particles with diameters larger than 10 nm, the penetration efficiency was higher than 95%, indicating minor losses of particles in the transfer line. The losses of VOCs in the transfer line were estimated to be less than 5%, which might lead to a small underestimation of SOA production."

Q2- The high, end of experiment SOA/POA ratios (Table 4) could largely be an artifact of substantial POA losses in the sampling system.

Reply: Conductive silicon tubes were used as sampling lines to reduce electrostatic losses of particles. In addition, the residence time of within seconds would also reduce the losses of particles. High SOA/POA ratios, mainly caused by the low concentrations of POA, might be related to the idling condition. Nordin et al. (2013) also observed high SOA/POA ratios and low concentrations of POA during the aging of emissions from idling Euro 2-4 light-duty gasoline vehicles.

The following text has been added to the revised manuscript.

"Conductive silicon tubes were used as sampling lines for HR-TOF-MS and SMPS to reduce electrostatic losses of particles."

Q3- This paper focuses on organic aerosol. What about total PM (that is what is regulated not organic aerosol)? Were there substantial refractory (e.g. BC) emissions?

Reply: Inorganic nitrate and ammonium were also formed synchronizing with SOA in some experiments. Formed nitrate mass could even reach 4–5 times as high as SOA. However, this paper mainly focused on organic aerosols, the formed inorganic aerosols will be discussed in detail in a subsequent paper. Theoretically, the difference of PM mass measured by AMS and SMPS should be attributed to black carbon. As

shown in Fig. S3 (Fig. 3 in the manuscript) in the SI, the initial mass of PM measured by SMPS was comparable with that measured by HR-TOF-AMS, thus we assumed that the mass of black carbon (BC) in the reactor was negligible.

The following text has been added to the revised manuscript.

"As shown in Fig. S3, the mass of primary particles measured by SMPS was comparable with that measured by HR-TOF-AMS, thus we assumed that the mass of black carbon (BC) in the reactor was negligible."

Q4- It does not appear that seed particles were used in the experiment. Therefore there is likely substantial loss of condensable vapors to the chamber walls (Zhang et al. PNAS 2014). This will reduce the SOA production.

Reply: The wall loss rate coefficient of vapors is related with the numbers of carbon and oxygen in the molecule (X. Zhang et al., 2015). Here, we take $C_7H_8O_4$, a product of the photo-oxidation of toluene as an example. The loss of $C_7H_8O_4$ to walls would be 7% in an hour before SOA formation when a wall deposition rate of 2×10^{-5} s^{-1} was used (X. Zhang et al., 2015). After SOA formation, the surface concentrations of particles increased fast to as high as 2000 μm^2 cm^{-3} in an hour, which would reduce the vapor wall losses. Therefore, the underestimation of SOA production due to vapor wall losses seems minor.

The following text has been added to the revised manuscript:

"Deposition of SOA-forming vapors to the walls might lead to the underestimation of SOA production. The wall loss rate coefficient of vapors is related with the numbers of carbon and oxygen in the molecule (X. Zhang et al., 2015). Here, we take $C_7H_8O_4$, a product of the photo-oxidation of toluene as an example. The loss of $C_7H_8O_4$ to walls would be 7% in an hour before SOA formation when a wall deposition rate of 2×10^{-5} s^{-1} was used (X. Zhang et al., 2015). After SOA formation, the surface concentrations of particles increased fast to as high as 2000 μm^2 cm^{-3} in an hour, which would reduce the vapor wall losses."

Q5- Blanks – Did they run any blank experiments (with no vehicle exhaust) to quantify contamination?

Reply: Blank experiments with no vehicle exhaust introduced were performed to

quantify the reactivity of the matrix gas. After 5 h of irradiation, the number and mass of formed particles were <5 cm^{-3} and 0.1 μg m^{-3}, respectively. Particle number distribution in a blank experiment was shown.

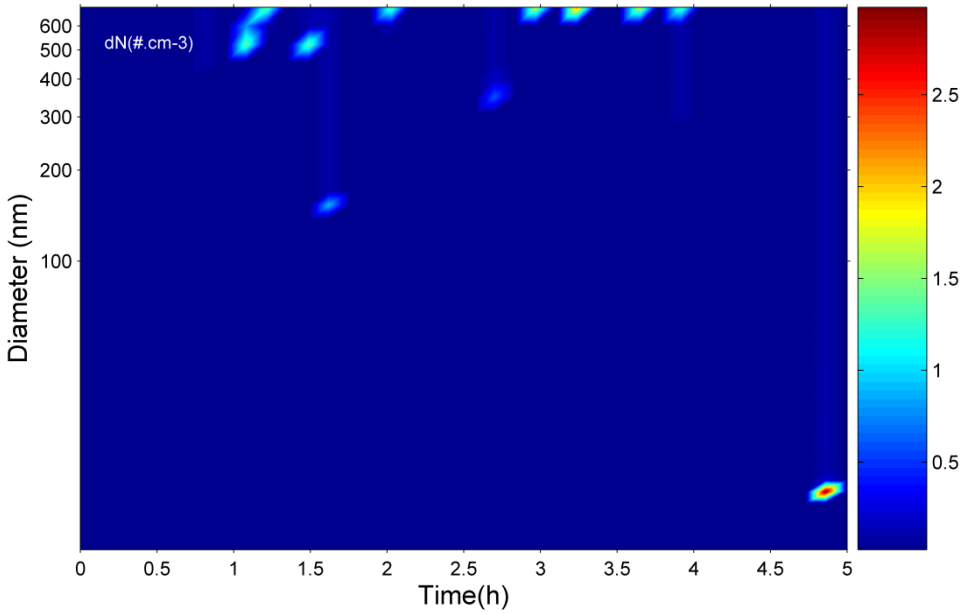

The following text has been added to the revised manuscript:

"Blank experiments with no vehicle exhaust introduced were performed to quantify the reactivity of the matrix gas. After 5 h of irradiation, the number and mass of formed particles were <5 cm^{-3} and 0.1 μg m^{-3}, respectively."

Q6- "alkanes shared about 42.9 and 66.2% of the total speciated NMHCs measured with the GC-FID/MSD by mass, respectively, dominating the NMHCs emissions in gasoline vehicle" not sure what "shared" means? Contributed might be a better word. It is not clear that alkanes dominate NMHC emissions, only NMHCs that were speciated in this study. This needs to be rephrased.

Reply: "shared" was changed to "*contributed*" as suggested in the revised manuscript. "dominating the NMHCs emissions" was changed to "*dominating the speciated VOCs emissions*" in the revised manuscript. NMHCs were changed to "*VOCs*" for purpose of consistency as suggested by referee 2.

Q7- "emission factors of NMHCs and aromatic hydrocarbons for vehicle I were 2.1 and 0.8 g kg^{-1}, approximately 1.3 and 0.5 times lower than those for vehicle II, respectively" Not clear what 0.5 times lower means. Does this mean the aromatic

emissions were actually higher for the newer vehicle. Also these seem like pretty modest emission reductions between a Euro 1 and a Euro 4 vehicle. I am not familiar with these specific standards but suspect that the expected reduction in NMHC emissions would be much greater than a factor of 2. This may reflect the fact that the experiments were performed at idle. Idle exhaust temperature are relatively low and therefore may not be sufficient to fully activate the catalytic converter. This further complicates interpreting the results (e.g. at idle, Euro 1 and Euro 4 vehicles may have similar emissions).

Reply: Emission factor of aromatics for Euro 4 vehicle was actually 43.5% of that for Euro 1 vehicle. This sentence has been changed in the revised manuscript and listed as follows: "The averaged emission factors of VOCs and aromatic hydrocarbons for Euro 4 vehicle were 2.1 and 0.8 g kg^{-1}, approximately 26.0% and 43.5% of those for Euro 1 vehicle, respectively." The VOCs emission factors based on g km^{-1} for Euro 1 and 4 vehicles were comparable with the previous reported values for Euro 1 and 4 gasoline vehicles in China (Huo et al., 2012; Huang et al., 2015). In this study, emission factors and compositions of VOCs for Euro 1 and 4 vehicles were significantly different.

The following text has been added to the revised manuscript.

"Using 7.87 L/100 km as the average fuel efficiency (Wagner et al., 2009), we obtained the VOCs emission factors based on g km^{-1} for Euro 4 and 1 vehicle to be 0.12 and 0.46 g km^{-1}, respectively, comparable with the previous reported values for Euro 1 and 4 gasoline vehicles in China (Huo et al., 2012; Huang et al., 2015). According to previous studies, there is a clear reduction of VOCs emissions from gasoline vehicles with stricter emission standards (Huo et al., 2012; Huang et al., 2015)."

Q8- " approximately 10 min, indicating dramatic new particle formation. After nucleation occured, the mean diameter increased from 20 to 60nm in about 1.5 h. Because particles with diameters lager than 50nm can act as cloud condensation nuclei (CCN) (McFiggans et al., 2006) and influence the radiative forcing, SOA from vehicle" The nucleation underscores the weakness of not having seed aerosol. The

reference to McFiggans and CCN is misleading since in the atmosphere there is substantial existing particle mass which will likely suppress nucleation of gasoline vehicle exhaust.

Reply: This issue was also mentioned by referee 2 (Q2). The starting surface concentrations of particles were all below a critical value (100–2000 μm^2 cm^{-3}) (Wehner et al., 2004), which benefited the formation of new particles. The sentence "*As shown in Fig. 5c, the total particle number concentration increased fast from 82 to 116143 cm^{-3} in approximately 10 min, indicating dramatic new particle formation. After nucleation occurred, the mean diameter increased from 20 to 60 nm). (Section 3.2, Page 10565, Line 11 – 17)"*has been revised and now reads:

"As shown in Fig. 3c, the total particle number concentration increased fast from 82 to 116143 cm^{-3}, indicating dramatic new particle formation, which might be due to that the starting surface concentrations of particles were all below a critical value (100–2000 μm^2 cm^{-3}, Table S1) (Wehner et al., 2004). As shown in Table S1, primary particle numbers in the reactor in this study ranged from 82 to 18948 cm^{-3}, 1-2 orders of magnitude higher than that of a Euro 2 car operated at idling with a similar dilution ratio (Nordin et al., 2013), indicating that the small starting particle number concentrations might mainly due to the idling condition of tested cars rather than the losses in the introduction lines. In addition, upon entering into the chamber, emitted particles would partition due to dilution similar as in the atmosphere, regardless of the temperature and concentration in the sampling system, which might lead to the decrease of starting number concentrations. A certain extent of primary particles under the detection limit of 14 nm of SMPS also contributed to the measured small starting number concentration of particles."

Q9- " aromatics and naphthalene accounted for 51–90% of the measured SOA, comparable to the estimation that classical C6–C9 light aromatics were" Claiming this level of mass closure is very problematic since they do not account for loss of condensable vapors to the walls. This seems more like the maximum amount of SOA they can explain.

Reply: We agree that this will be the maximum amount of SOA can be explained if

wall losses of condensable vapors are not accounted for. If we take $C_7H_8O_4$ as an example, a maximum underestimation of SOA production due to wall losses of organic vapors throughout the experiments would be 30%, single-ring aromatics and naphthalene would thus account for 43%-80% of the measured SOA. This will not change the conclusion that aromatics and naphthalene are main SOA precursors in LDGV exhausts. The following text has been added to the revised manuscript.

"Wall losses of organic vapors were not considered in this study, which would lead to the underestimation of SOA production. Therefore, the mass closure analysis estimated the maximum amount of SOA that could be explained by aromatics."

Q10- "The wall-loss rate constant was determined separately for each experiment by fitting the SMPS and AMS data when no new particles were formed." I do not understand this. No new particles formed suggests to me no nucleation. I suspect they mean before there is any photo-oxidation – needs to be clarified in the text.

Reply: SMPS and AMS data were fit with first-order kinetics after UV lamps were turned off. This sentence has been changed to "The wall-loss rate constant was determined separately for each experiment by fitting the SMPS and AMS data with first-order kinetics when UV lamps were turned off." in the revised manuscript.

Q11- "The w = 1 wall-loss correction is not suitable for the experiments here in which nucleation occurred and no seed particles were added" I do not understand why this is the case. The ~1 hr induction period before SOA formation could simply reflect loss of condensable vapors to the walls. I can understand why the w=1 case may not be representative of the vapor losses, but it seems incorrect (based on the results of Zhang) to ignore the wall losses of vapors. Also, wall losses with vapors will mean that you likely underestimate the amount of SOA production and therefore that your mass closure analysis estimates the maximum amount of SOA that can be explained with single ring aromatics.

Reply: For the case ω=1, the following equation is used to constrain the vapor wall loss (Hildebrandt et al., 2009).

$$C_{OA}(t) = \frac{C_{OA}^{sus}(t)}{C_{seed}^{sus}(t)} C_{seed}^{sus}(t=0)$$

Suspended seed particles are needed to correct the vapor wall loss. Thus the ω= 1 wall-loss correction is not suitable for the experiments in which no seed particles are added. 1 h introduction period would lead to around 7% loss of organic vapor to walls if we took $C_7H_8O_4$ as an example. The subsequently formed SOA, with surface concentrations as high as 2000 μm^2 cm^{-3}, provided condense sinks to reduce the vapor wall losses.

Q12- "Table 5. Chemical compositions of the aromatic hydrocarbons in the exhaust of different vehicles, listed as weight percentages." Weight percentages of what? Speciated NMHCs?

Reply: Additional information in Table 5 was added to Figure 4, now Fig. 2 in the revised manuscript, as suggested by referee 2. Chemical compositions were presented as weight percentages of speciated NMHCs, this has been clarified in the caption of Fig. 2.

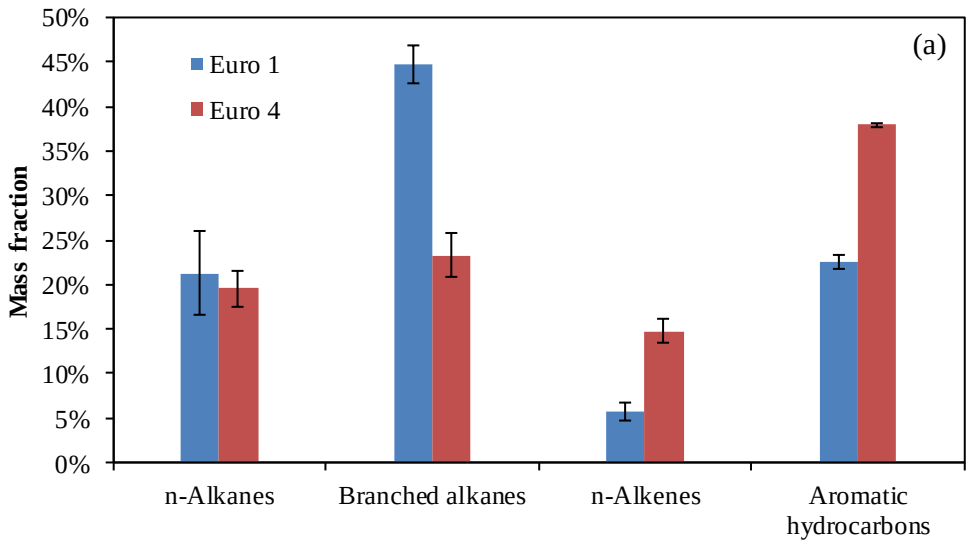

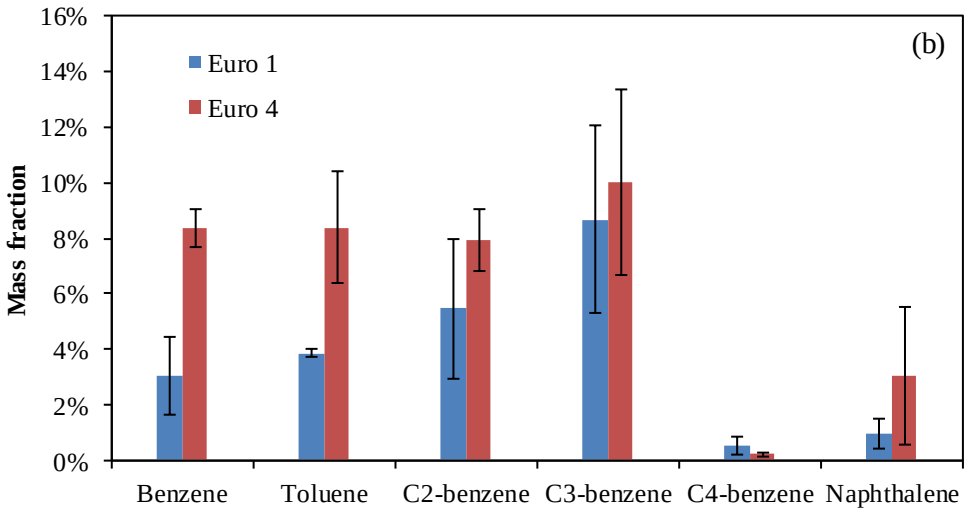

Q13- Figure 2. Particle number (left) and mass (right) distributions for a typical smog chamber experiment (experiment). The right hand panel suggests that there is substantial mass in the nucleation mode (much more than the 3% suggested in the text). Wall loss of these very small particles is more rapid than the larger particles. How was this corrected for?

Reply: Nucleation mode only includes particles with diameters smaller than 20 nm. Less than 3% of the particle mass is in the nucleation mode ten minutes after nucleation for all the experiments. The SOA formation is sufficiently fast (~ 1 h) and the particle volume distribution shifted not much after SOA reached the maximum value in about 1 h. Therefore, the impact of the nucleation event on wall-loss estimate is considered to be negligible as other nucleation studies did (Cocker et al. 2001; Pathak et al., 2007). In addition, Keywood et al. (2004) concluded that particle wall loss rates could not be accurately quantified for those particles generated in a nucleation event.

Q14- Figure 4 – Mass fraction of what?

Reply: Mass fraction of speciated NMHCs. This has been clarified in the caption.

Q15- Figure 6. They attribute lower yields measured here compared to Nordin et al. to not using seed particles, which leads to higher losses of vapors to the smog chamber walls. That seems like a reasonable explanation. If that is the case then the amount of unexplained SOA is twice what they report. This caveat needs to be included in the text. Also, did Nordin have the same or higher OH exposures. This

might also impact the yield.

Reply: The existence of seed particles in the study of Nordin et al. (2013) might reduce the wall loss of semi-volatile organic vapors and thus increase the effective SOA yield (Kroll et al., 2007; Zhang et al., 2014; X. Zhang et al., 2015). However, Cocker et al. (2001) found that SOA formation from m-xylene and 1,3,5-trimethylbenzene photo-oxidation was unaffected by the presence of ammonium sulfate seed aerosols. The influence of seed particles on SOA yields still needs further investigations. Higher OH concentrations in the study of Nordin et al. (2013) would also result in higher SOA yields (Ng et al., 2007). The discussion in the manuscript has been rewritten and now reads:

"The effective SOA yields in the study of Nordin et al. (2013) were 60%-360% higher than those in this study at same concentrations of M_0. In their calculation of the reacted SOA precursors, C4-benzene and naphthalene were excluded. The effective SOA yields would increase 7%-34% when C4-benzene and naphthalene were excluded in this study, which could explain a small portion of the discrepancy. According to the estimation above, the loss of VOCs in the transfer lines was less than 5%. A little higher than VOCs, if assumed to be 20%, losses of IVOCs and SVOCs in the transfer lines would increase the SOA effective yields by a factor of 2%-10% when the unexplained SOA discussed later was all attributed to the contribution from IVOCs and SVOCs. The existence of seed particles in the study of Nordin et al. (2013) might reduce the wall loss of semi-volatile organic vapors and thus increase the effective SOA yield (Kroll et al., 2007; Zhang et al., 2014; X. Zhang et al., 2015). However, Cocker et al. (2001) found that SOA formation from m-xylene and 1,3,5-trimethylbenzene photo-oxidation was unaffected by the presence of ammonium sulfate seed aerosols. The influence of seed particles on SOA yields still needs further investigations. Faster oxidation rates caused by higher OH concentrations in the study of Nordin et al. (2013) would also result in higher SOA yields (Ng et al., 2007)."

Q16- The effective yields are defined based on a relatively small number of single ring aromatics. Did Nordin use the same set of compounds to define their effective yield? If not, is it fair to compare the new results with Nordin et al. results based on

yields. The fact that the effective yield was defined relative to this small subset of compounds needs to more clearly stated in paper, including the presentation of the effective yield results and in the caption of Figure 6.

Reply: In the study of Nordin et al. (2013), C4-benzene and naphthalene were excluded when calculating the mass of reacted SOA precursors. The effective SOA yields would increase 7%-34% when C4-benzene and naphthalene were excluded in this study, which could explain a small portion of the discrepancy. The calculation of effective yield has been stated in section "2.4.3 Effective SOA yields" and in the caption of Fig. 4 in the revised manuscript.

Q17- Figure 7 – is this just plotting numbers in Table 3? If so, Table 3 could go into the supplemental.

Reply: Table 3 has been moved to SI.

Q18- Given that they only have two vehicles; I would refer to them in the text by their certification standard, not Vehicle 1 and Vehicle 2. I had to keep looking up which one is which.

Reply: As suggested the tested vehicles were presented as Euro 1 and Euro 4 throughout the revised manuscript.

Q19- "In this study, the SOA yield of benzene and other single-ring aromatics were estimated using the two-product model curves taken from Borrás et al. (2012) and Odum et al. (1997), respectively. While the SOA yield of naphthalene was taken from Shakya et al. (2010)." How representative are these yields of the rest of the literature. E.g. I think that the Odum yields are on the low end of the literature yields for single ring aromatic (in part because they did not use seed aerosols). Do conclusions about the mass closure change if the analysis is done with different yields. Were the yields taken from the literature measured under similar experimental conditions as these experiments (e.g. VOC/NO_x, OA concentration). Given the uncertainty in the yields, the analysis should be repeated with different published yield data to generate error bars in the mass closure estimates (51 to 90%).

Reply: In the study of Odum et al. (1997), around 5000 to 10000 cm^{-3}, 5–10 μm^3 cm^{-3} of ammonium sulfate were introduced as seed aerosols. The adoption of SOA yield

curves of toluene and m-xylene from Ng et al. (2007) would increase the mass closure estimation to 55%-114%. But the experimental conditions of Ng et al. (2007) were quite different from this study. In the study of Ng et al. (2007), about 10000 cm^{-3} and 15 μm^3 cm^{-3} of ammonium sulfate served as seed aerosols. In addition, nitrous acid was used as OH precursor to provide higher oxidation rates, resulting in higher SOA yields. Therefore, the SOA yield curves of Ng et al. (2007) were not suitable for this study. Considering that the study of Odum et al. (1997) provided a systematic estimation of SOA yields from toluene, C2-benzene, C3-benzene and C4-benzene, we mainly used the two-product curves from Odum et al. (1997) to estimate the SOA production. The following text has been added to the revised manuscript.

"SOA yield curves of toluene and m-xylene from Ng et al. (2007) were also widely used to estimate SOA production (Platt et al., 2013). However, the introduction of seed aerosols and OH precursor made the SOA yield curves in the study of Ng et al. (2007) not suitable for this study. Considering that the study of Odum et al. (1997) provided a systematic estimation of SOA yields from toluene, C2-benzene, C3-benzene and C4-benzene, we mainly used the two-product curves from Odum et al. (1997) to estimate the SOA production."

Q20- Page 10555 line 15 – "form" should be "from"

Reply: Revised as suggested.

Q21- Table 2 – Is this supposed to be ppbv carbon for NMHCs?

Reply: It is just ppbv instead of ppbv carbon.

References

Cocker Iii, D. R., Mader, B. T., Kalberer, M., Flagan, R. C., and Seinfeld, J. H.: The effect of water on gas–particle partitioning of secondary organic aerosol: II. m-xylene and 1,3,5-trimethylbenzene photooxidation systems, Atmos. Environ. 2001, 35, 6073-6085.

Gormley, P. G., and Kennedy, M.: Diffusion from a Stream Flowing through a Cylindrical Tube, Proceedings of the Royal Irish Academy. Section A: Mathematical and Physical Sciences1949, 52, 163-169.

Hildebrandt, L., Donahue, N. M., and Pandis, S. N.: High formation of secondary organic aerosol from the photo-oxidation of toluene, Atmos. Chem. Phys. 2009, 9, 2973-2986.

Huang, C., Wang, H. L., Li, L., Wang, Q., Lu, Q., de Gouw, J. A., Zhou, M., Jing, S. A., Lu, J., and Chen, C. H.: VOC species and emission inventory from vehicles and their SOA formation potentials estimation in Shanghai, China, Atmos. Chem. Phys. Discuss. 2015, 15, 7977-8015.

Huo, H., Yao, Z., Zhang, Y., Shen, X., Zhang, Q., Ding, Y., and He, K.: On-board measurements of emissions from light-duty gasoline vehicles in three mega-cities of China, Atmos. Environ. 2012, 49, 371-377.

Keywood, M. D., Varutbangkul, V., Bahreini, R., Flagan, R. C., and Seinfeld, J. H.: Secondary Organic Aerosol Formation from the Ozonolysis of Cycloalkenes and Related Compounds, Environ. Sci. Technol. 2004, 38, 4157–4164.

Kroll, J. H., Chan, A. W. H., Ng, N. L., Flagan, R. C., and Seinfeld, J. H.: Reactions of Semivolatile Organics and Their Effects on Secondary Organic Aerosol Formation, Environ Sci Technol. 2007, 41, 3545-3550.

Liu, T. Y., Wang, X. M., Wang, B. G., Ding, X., Deng, W., Lü, S. J., and Zhang, Y. L.: Emission factor of ammonia (NH_3) from on-road vehicles in China: tunnel tests in urban Guangzhou, Environ. Res. Lett. 2014, 9, 064027.

National Bureau of Statistics of China: China Statistical Yearbook, Beijing: China Statistics Press, 2013.

Ng, N. L., Kroll, J. H., Chan, A. W. H., Chhabra, P. S., Flagan, R. C., and Seinfeld, J. H.: Secondary organic aerosol formation from m-xylene, toluene, and benzene, Atmos. Chem. Phys. 2007, 7, 3909-3922.

Nordin, E. Z., Eriksson, A. C., Roldin, P., Nilsson, P. T., Carlsson, J. E., Kajos, M. K., Hellén, H., Wittbom, C., Rissler, J., Löndahl, J., Swietlicki, E., Svenningsson, B., Bohgard, M., Kulmala, M., Hallquist, M., and Pagels, J. H.: Secondary organic aerosol formation from idling gasoline passenger vehicle emissions investigated in a smog chamber, Atmos. Chem. Phys. 2013, 13, 6101-6116.

Odum, J. R., Jungkamp, T. P. W., Griffin, R. J., Forstner, H. J. L., Flagan, R. C., and

Seinfeld, J. H.: Aromatics, reformulated gasoline, and atmospheric organic aerosol formation, Environ. Sci. Technol. 1997, 31, 1890-1897.

Platt, S. M., El Haddad, I., Zardini, A. A., Clairotte, M., Astorga, C., Wolf, R., Slowik, J. G., Temime-Roussel, B., Marchand, N., Ježek, I., Drinovec, L., Močnik, G., Möhler, O., Richter, R., Barmet, P., Bianchi, F., Baltensperger, U., and Prévôt, A. S. H.: Secondary organic aerosol formation from gasoline vehicle emissions in a new mobile environmental reaction chamber, Atmos. Chem. Phys. 2013, 13, 9141-9158.

Schauer, J. J., Kleeman, M. J., Cass, G. R., and Simoneit, B. R. T.: Measurement of emissions from air pollution sources. 5. C1−C32 organic compounds from gasoline-powered motor vehicles, Environ. Sci. Technol. 2002, 36, 1169-1180.

Wagner, D. V., An, F., and Wang, C.: Structure and impacts of fuel economy standards for passenger cars in China, Energy Policy 2009, 37, 3803-3811.

Wehner, B., Wiedensohler, A., Tuch, T. M., Wu, Z. J., Hu, M., Slanina, J., and Kiang, C. S.: Variability of the aerosol number size distribution in Beijing, China: New particle formation, dust storms, and high continental background, Geophys. Res. Lett. 2004, 31, L22108.

Zhang, X., Cappa, C. D., Jathar, S. H., McVay, R. C., Ensberg, J. J., Kleeman, M. J., and Seinfeld, J. H.: Influence of vapor wall loss in laboratory chambers on yields of secondary organic aerosol, Proceedings of the National Academy of Sciences, 10.1073/pnas.1404727111, 2014.

Zhang, X., Schwantes, R. H., McVay, R. C., Lignell, H., Coggon, M. M., Flagan, R. C., and Seinfeld, J. H.: Vapor wall deposition in Teflon chambers, Atmos. Chem. Phys. 2015, 15, 4197-4214.

Zhang, Y., Wang, X., Zhang, Z., Lü, S., Shao, M., Lee, F. S. C., and Yu, J.: Species profiles and normalized reactivity of volatile organic compounds from gasoline evaporation in China, Atmos. Environ. 2013, 79, 110-118.

Zhang, Y. L., Wang, X. M., Li, G. H., Yang, W. Q., Huang, Z. H., Zhang, Z., Huang, X. Y., Deng, W., Liu, T. Y., Huang, Z. Z., and Zhang, Z. Y.: Emission factors of fine particles, carbonaceous aerosols and traces gases from road vehicles: recent tests in an urban tunnel in the Pearl River Delta, China, Atmos. Environ. 2015 (revised).

Response to Reviewer #2

General Remarks:

The manuscript fits the scope of the journal and is of scientific relevance to the community. As the manuscript title suggests, the study provides insight into organic aerosols as emitted primarily from gasoline vehicles (1x Euro 4 and 1x Euro 1) and reports on the secondarily formed organic aerosol (SOA) mass upon photo oxidation in a smog chamber. The tested gasoline vehicles are operated in China with Euro III compliant gasoline fuel. Modern state-of-the art instrumentation is used in the investigations. The article is well structured, and provides additional data for the community, adding to the statistics on gasoline vehicle SOA formation. This is of significance, as previous publications (Nordin et al., 2013, Platt et al., 2013, Platt et al., 2014, Gordon et al., 2014, May et al. 2013ab, and others) have shown large error bars on gasoline vehicle SOA formation estimations, and additional data help to constrain gasoline vehicle SOA formation further. However, I disagree with the repeated statements in the abstract, introduction and conclusions, that these experiments are representative of Chinese vehicles compared to previous experiments, due to (1) limited experimental conditions, and (2) the limited number of tests conducted (5 tests with 2 vehicles). However, in general, the results lie within previous findings (note that I do feel that an extended comparison with existing literature is recommended, see references mentioned above) and support the overall statistical quality of the data, despite the fact, that no significantly new conclusions are found. I believe before publication the authors should clearly state that the numbers reported are only valid for the tested cars and more data would be required to constrain the Chinese vehicular emissions.

Reply: As shown in the revised manuscript, aromatic hydrocarbons contributed 22.5%-38% of the total VOCs for idling conditions in this study, within the ranges of tunnel measurements and those measured under ECE and FTP urban driving conditions (Schauer et al., 2002; Gentner et al., 2013; Wang et al., 2013). Thus the composition of exhausts for our idling case is of relevance for gasoline vehicle

emissions. Yes, our manuscript just provided valuable additional data to the statistics on gasoline vehicle SOA formation. As replying to another reviewer, we admit that number of tests is quite limited. We have mentioned this in the revised manuscript.

Specific Remarks: Experimental Methods and Data Analysis:

While the data support the current literature, the experimental methods and sample size lead to limited results that are not globally representative and should not be used to draw global conclusions, e.g. on the vehicle fleet in China. The reason for stating the limited scope of the study is, that it relies on replicates (2 - 3x) of only two measurements of idling gasoline vehicles (1x Euro 4, 1x Euro 1), excluding the influence of different driving behavior and technologies. In addition, problems with the experimental set-up and the data processing have to be pointed out. The following major points regarding the experimental set up and data analysis must be addressed before I could recommend publication:

Q1- Sampling lines were unheated Teflon, and samples were taken through a pump: this will lead to losses of (1) primary particles through electrostatic losses, and (2) VOCs, IVOCs and $SVOC_S$ via adsorption on the Teflon surface; In addition, there might be significant losses in the pump. Could the authors add estimations for particle and gas-phase losses in the sampling system, or give more information on the operation of the pump and how this will affect the sample taken into the smog chamber? (Losses are potentially indicated by the small starting particle number concentration in the smog chamber). Please provide starting concentrations in SI.

Reply: We agree that losses in unheated transfer lines are important considerations. Therefore, a flow rate of as high as 20 L min^{-1} and a transfer line of as short as 5 m were used to provide residence time within seconds, and thus reduce the losses of particles and VOCs in the transfer lines. Furthermore, before being introduced into the reactor, gasoline vehicle exhausts were generally pumped through the transfer lines for half an hour to saturate the transfer lines with particles and VOCs while warming the catalytic converter. Losses of particles and VOCs in the introduction lines were determined by comparing the concentrations of total particle number and VOCs in the

directly emitted exhausts and the ones after passing through the transfer lines. As shown in Figure 1, the distributions of particle number in the directly emitted exhausts and the ones after passing through the transfer lines were similar. The loss of total particle number was estimated to be less than 3%. The penetration efficiency of particles in the transfer line was also estimated by a laminar diffusional deposition model (Gormley and Kennedy, 1949). For particles with diameters larger than 10 nm, the penetration efficiency was higher than 95%, indicating minor losses of particles in the transfer line. The losses of VOCs in the transfer line were estimated to be less than 5%, which might lead to a small underestimation of SOA production. The initial particle number concentrations were provided in SI. Primary particle numbers in the reactor in this study ranged from 82 to 18948 cm^{-3}, 1-2 orders of magnitude higher than that of a Euro 2 car operated at idling with a similar dilution ratio (Nordin et al., 2013), indicating that the small starting particle number concentration might mainly due to the idling condition of tested cars rather than the losses in the introduction lines. In addition, upon entering into the chamber, emitted particles would partition due to dilution similar as in the atmosphere, regardless of the temperature and concentration in the sampling system, which might lead to the decrease of starting number concentrations. A certain extent of primary particles under the detection limit of 14 nm of SMPS also contributed to the measured small starting number concentration of particles.

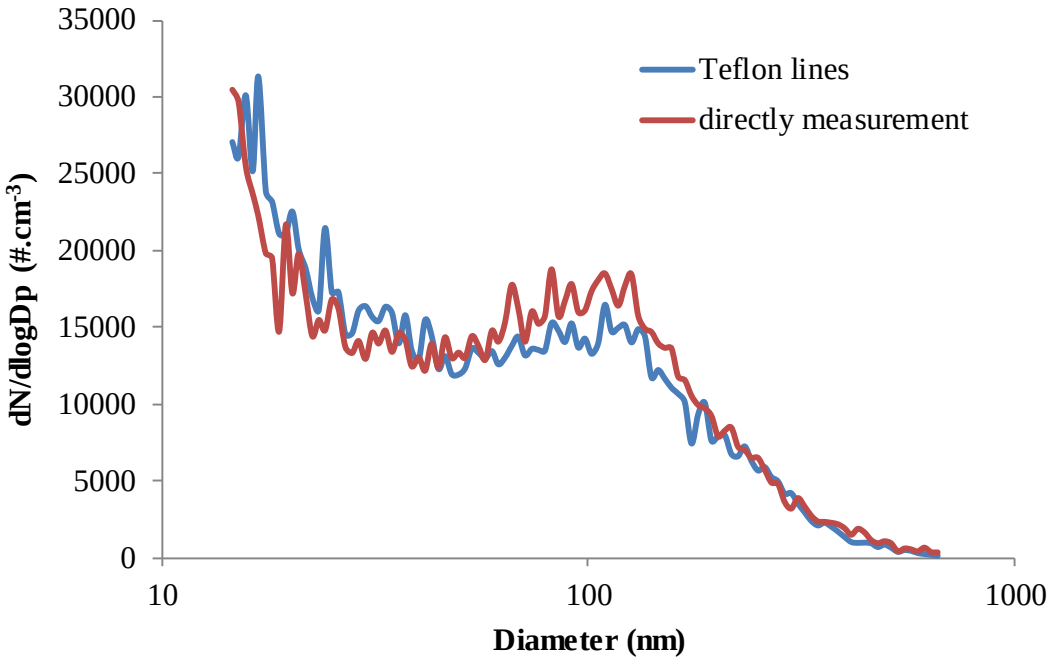

Figure 1. Particle number distributions of the directly emitted exhausts and the ones after passing through the transfer lines.

The following text has been added to the revised manuscript.

"During the introduction of exhausts, particles and VOCs might deposit to the surface of the transfer lines. Therefore, a flow rate of as high as 20 L min^{-1} and a transfer line of as short as 5 m were used to provide residence time within seconds, and thus reduce the losses of particles and VOCs in the transfer lines. Furthermore, before being introduced into the reactor, exhausts were generally pumped through the transfer lines for half an hour to saturate the transfer lines with particles and VOCs while warming the catalytic converter. Losses of particles and VOCs in the introduction lines were determined by comparing the concentrations of total particle number and VOCs in the directly emitted exhausts with the ones after passing through the transfer lines. The loss of total particle number was estimated to be less than 3%. The penetration efficiency of particles due to diffusion in a cylindrical tube, η(dp), can be also estimated by a laminar diffusional deposition model (Gormley and Kennedy, 1949). For particles with diameters larger than 10 nm, the penetration efficiency was higher than 95%, indicating minor losses of particles in the transfer line. The losses of VOCs in the transfer line were estimated to be less than 5%, which

might lead to a small underestimation of SOA production."

Q2- Nucleation is observed upon photooxidation, which points to the fact that there was not enough seed aerosol surface available in the smog chamber; potential losses of vapors to chamber walls should be taken into account. Can the authors estimate the starting seed aerosol surface? (Section 3.2, Page 10565, Line 11 – 17, "As shown in Fig. 5c, the total particle number concentration increased fast from 82 to 116143 cm^{-3} in approximately 10 min, indicating dramatic new particle formation. After nucleation occurred, the mean diameter increased from 20 to 60 nm)."

Reply: As shown in the Table below, which is now the Table S1 in SI, the starting surface concentrations of particles were all below a critical value (100–2000 μm^2 cm^{-3}) (Wehner et al., 2004), which benefited the formation of new particles. The wall loss rate coefficient of vapors is related with the numbers of carbon and oxygen in the molecule (X. Zhang et al., 2015). Here, we take $C_7H_8O_4$, a product of the photo-oxidation of toluene as an example. The loss of $C_7H_8O_4$ to walls would be 7% in an hour before SOA formation when a wall deposition rate of 2×10^{-5} s^{-1} was used (X. Zhang et al., 2015). After SOA formation, the surface concentrations of particles increased fast to as high as 2000 μm^2 cm^{-3} in an hour, which would reduce the vapor wall losses. The sentence "*As shown in Fig. 5c, the total particle number concentration increased fast from 82 to 116143 cm^{-3} in approximately 10 min, indicating dramatic new particle formation. After nucleation occurred, the mean diameter increased from 20 to 60 nm). (Section 3.2, Page 10565, Line 11 – 17)"*has been revised and now reads:

"As shown in Fig. 3c, the total particle number concentration increased fast from 82 to 116143 cm^{-3}, indicating dramatic new particle formation, which might be due to that the starting surface concentrations of particles were all below a critical value (100–2000 μm^2 cm^{-3}, Table S1) (Wehner et al., 2004). As shown in Table S1, primary particle numbers in the reactor in this study ranged from 82 to 18948 cm^{-3}, 1-2 orders of magnitude higher than that of a Euro 2 car operated at idling with a similar dilution ratio (Nordin et al., 2013), indicating that the small starting particle number concentrations might mainly due to the idling condition of tested cars rather than the

losses in the introduction lines. In addition, upon entering into the chamber, emitted particles would partition due to dilution similar as in the atmosphere, regardless of the temperature and concentration in the sampling system, which might lead to the decrease of starting number concentrations. A certain extent of primary particles under the detection limit of 14 nm of SMPS also contributed to the measured small starting number concentration of particles.

Deposition of SOA-forming vapors to the walls might lead to the underestimation of SOA production. The wall loss rate coefficient of vapors is related with the numbers of carbon and oxygen in the molecule (X. Zhang et al., 2015). Here, we take $C_7H_8O_4$, a product of the photo-oxidation of toluene as an example. The loss of $C_7H_8O_4$ to walls would be 7% in an hour before SOA formation when a wall deposition rate of 2 $\times 10^{-5}$ s^{-1} was used (X. Zhang et al., 2015). After SOA formation, the surface concentrations of particles increased fast to as high as 2000 μm^2 cm^{-3} in an hour, which would reduce the vapor wall losses."

Table S1. The initial number and surface concentrations of particles at t = 0 h (since lights on) in each experiment.

Experiment #	Number (cm^{-3})	Surface (μm^2 cm^{-3})
1	114	2.23
2	82	2.9
3	332	4.7
4	337	4.2
5	18948	25.8

Q3- Problems with the AMS/SMPS analysis are indicated: Figure 2 presents SMPS size distribution from a HR-ToF-AMS. Likely a big fraction of the mass as measured with the HR-ToF-AMS is actually outside the optimum transmission efficiency of the lens. No direct correction for lens transmission was applied, but the authors scaled AMS data with SMPS data. However, lens transmission issues are not discussed in section 2.2. and 2.4.2. I recommend adding this to the manuscript. Additionally, I would like to ask the authors to clarify how refractory particulate matter (elemental carbon) has been taken into account in the analysis, or discuss, why it was assumed

that the vehicle exhaust studied in the smog chamber consist only of non-refractory material.

Reply: Figure 2 (to be included in SI as Fig. S2) shows the particle volume distribution measured by SMPS for a typical smog chamber experiment (experiment 2). As shown, most particles were in the range 40-120 nm after SOA formation. Since the transmission window of the standard lens of HR-TOF-AMS is 60-600 nm (aerodynamic diameter) (Liu et al., 2007), particles with diameter lower than 40 nm (mobility diameter) were cut from the lower edge of the volume distribution. After 1 h since nucleation occurred, only <5% of the mass was outside the transmission window of HR-TOF-MS, indicating that HR-TOF-AMS might underestimate the PM in the early stage of SOA formation.

The following text has been added to the revised manuscript.

"Fig. S2 shows the particle volume distribution measured by SMPS for a typical smog chamber experiment (experiment 2). Most particles were in the range 40-120 nm after SOA formation. Since the transmission window of the standard lens of HR-TOF-AMS is 60-600 nm (aerodynamic diameter) (Liu et al., 2007), particles with diameter lower than 40 nm (mobility diameter) were cut from the lower edge of the volume distribution. After 1 h since nucleation occurred, only <5% of the mass was outside the transmission window of HR-TOF-MS, indicating that HR-TOF-AMS might underestimate the PM in the early stage of SOA formation."

Theoretically, the difference of PM mass measured by AMS and SMPS should be attributed to black carbon. As shown in Fig. S3 in the SI, the initial mass of PM measured by SMPS was comparable with that measured by HR-TOF-AMS, thus we assumed that the mass of black carbon (BC) in the reactor was negligible.

The following text has been added to the revised manuscript.

"As shown in Fig. S3, the mass of primary particles measured by SMPS was comparable with that measured by HR-TOF-AMS, thus we assumed that the mass of black carbon (BC) in the reactor was negligible."

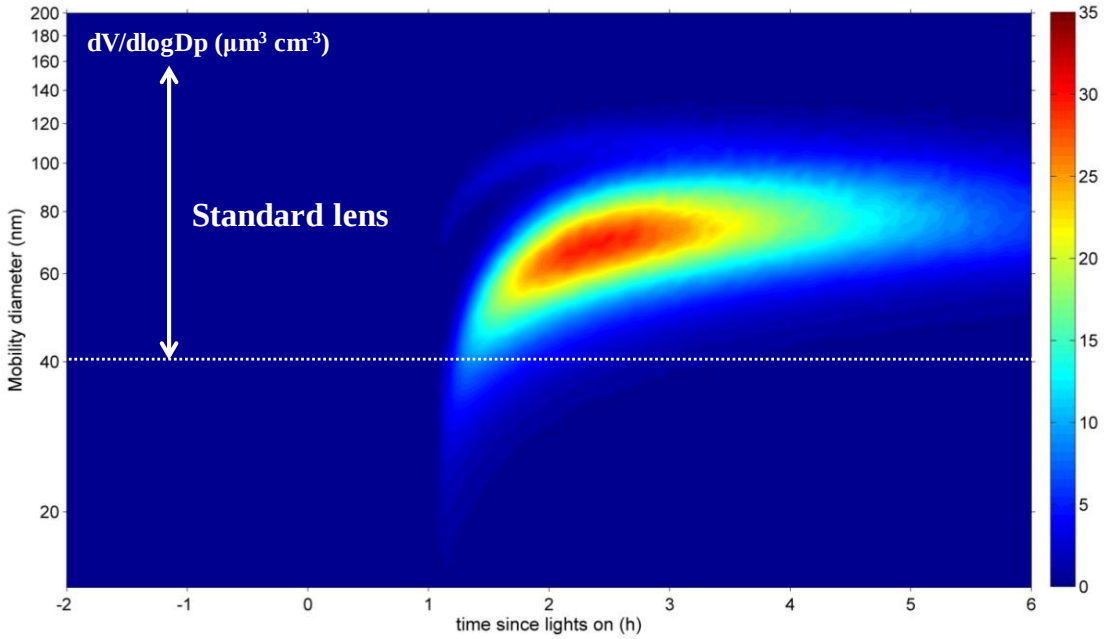

Figure 2. Particle volume distribution measured by SMPS for a typical smog chamber experiment (experiment 2).

Q4- Offline samples were taken with different systems (e.g. aluminum foil bags, stainless steel containers). Please clarify which systems were applied when, and which analysis was performed. I expect significant losses for SOA precursors on stainless steel surfaces (see e.g. section 2.4.3, page 10563, line 13). Did results from offline samples compare well with online PTR-ToF-MS results (please add this to section 3.1).

Reply: Raw exhausts were collected into aluminum foil bags with VOCs and CO_2 analyzed to characterize the primary emissions from exhaust pipe. At the beginning and end of each experiment, air samples in the reactor were collected into evacuated 2 L stainless steel canisters and analyzed by GC-MSD to determine the mass of reacted organic precursors. The sampling and analysis methods have been clarified in the revised manuscript. The inner surfaces of the canisters has been electropolished and passivated to eliminate absorption of VOCs. This method has been widely used to collect VOCs samples (Barletta et al., 2005). In addition, samples in canisters were analyzed immediately after collection. We believe that our sampling and analysis methods accurately measure VOCs in the chamber. The text "evacuated 2 L stainless

steel canisters" has been revised to "*2 L electropolished and evacuated stainless steel canisters*" in the revised manuscript.

In this study, GC-MS was the standard method to determine the mass concentrations of single-ring aromatics. PTR-TOF-MS was used for deriving the time-resolved concentrations of single-ring aromatics. In addition, the VOC concentrations measured offline were also used as an independent check of that measured online by the PTR-TOF-MS. The following text has been added to the revised manuscript to clarify:

"In this study, the offline measurement was the standard method to determine the mass concentrations of VOCs. PTR-TOF-MS was used for deriving the time-resolved concentrations of VOCs."

Q5- Estimation of yields: Relatively low yields are found (3–17%), compared to previous publications on gasoline vehicles tested on driving cycles. Please provide extended discussion on potential reasons, and clarify how significant losses of IVOCs and SVOCs compared to VOCs in the unheated Teflon lines used for sample introduction and in the stainless steel containers used for sample collection would skew these results.

Reply: The effective SOA yields in the study of Nordin et al. (2013) were 60%-360% higher than those in this study at same concentrations of M_0. In their calculation of the reacted SOA precursors, C4-benzene and naphthalene were excluded. The effective SOA yields would increase 7%-34% when C4-benzene and naphthalene were excluded in this study, which could explain a small portion of the discrepancy. According to the estimation above, the loss of VOCs in the transfer lines was less than 5%. A little higher than VOCs, if assumed to be 20%, losses of IVOCs and SVOCs in the transfer lines would increase the SOA effective yields by a factor of 2%-10% when the unexplained SOA discussed later was all attributed to the contribution from IVOCs and SVOCs. The existence of seed particles in the study of Nordin et al. (2013) might reduce the wall loss of semi-volatile organic vapors and thus increase the effective SOA yield (Kroll et al., 2007; Zhang et al., 2014; X. Zhang et al., 2015). However, Cocker et al. (2001) found that SOA formation from m-xylene and

1,3,5-trimethylbenzene photo-oxidation was unaffected by the presence of ammonium sulfate seed aerosols. The influence of seed particles on SOA yields still needs further investigations. The discussion in the manuscript has been rewritten and now reads:

"The effective SOA yields in the study of Nordin et al. (2013) were 60%-360% higher than those in this study at same concentrations of M_0. In their calculation of the reacted SOA precursors, C4-benzene and naphthalene were excluded. The effective SOA yields would increase 7%-34% when C4-benzene and naphthalene were excluded in this study, which could explain a small portion of the discrepancy. According to the estimation above, the loss of VOCs in the transfer lines was less than 5%. A little higher than VOCs, if assumed to be 20%, losses of IVOCs and SVOCs in the transfer lines would increase the SOA effective yields by a factor of 2%-10% when the unexplained SOA discussed later was all attributed to the contribution from IVOCs and SVOCs. The existence of seed particles in the study of Nordin et al. (2013) might reduce the wall loss of semi-volatile organic vapors and thus increase the effective SOA yield (Kroll et al., 2007; Zhang et al., 2014; X. Zhang et al., 2015). However, Cocker et al. (2001) found that SOA formation from m-xylene and 1,3,5-trimethylbenzene photo-oxidation was unaffected by the presence of ammonium sulfate seed aerosols. The influence of seed particles on SOA yields still needs further investigations. Faster oxidation rates caused by higher OH concentrations in the study of Nordin et al. (2013) would also result in higher SOA yields (Ng et al., 2007)."

Specific Remarks: Language / Formulations:

Q6-Abstract: - Please remove the sentence "However, there are still no chamber simulation studies in China on SOA formation from vehicle exhausts" (Line 4-5) as it is not of significance in which country laboratory experiments are performed.

Reply: revised as suggested.

Q7- Please add "operated" to "in China" in Line 7, so that the sentence reads ". . . operated in China . . ."

Reply: revised as suggested.

Q8-Please reformulate "at the quite similar OH exposure" to "at comparable OH

exposure".

Reply: revised as suggested.

Q9-Section 1, Introduction: - Section 1, Page 10557, Line 13: please reformulate or remove; see comments on Abstract.

Reply: The sentence has been removed and now the paragraph reads: "In China, the number of LDGVs reached 98.8 million in 2012 and increased……"

Q10- Section 1, Page 10557, Line 26, please reformulate; see comments on Abstract.

Reply: Revised as "*operated in China*".

Q11- Section 2, Materials and methods: - Please add a section on derivation of OH exposure to Materials and methods.

Reply: A section on the derivation of OH exposure has been added to the revised manuscript as below:

"Decay of toluene measured by PTR-TOF-MS is used to derive the average OH concentration during each experiment. Changes in the toluene concentration over time can be expressed as:

$$\frac{d[toluene]}{dt} = -k \cdot [OH] \cdot [toluene] \qquad (3)$$

where k is the rate constant for the reaction between toluene and OH radical. Assuming a constant OH concentration during an experiment, we can integrate Eq. (3) to get Eq. (4):

$$\ln(\frac{[toluene]_0}{[toluene]_t}) = k \cdot [OH] \cdot t \qquad (4)$$

So by plotting $ln([toluene]_0/[toluene]_t)$ versus time t, we can obtain a slope that equals $k \times [OH]$. The average OH concentration is therefore calculated as:

$$[OH] = \frac{slope}{k} \qquad (5)$$

The OH exposure is then determined through multiplying the average OH

concentration by time."

Q12- Section 2.4.2., please move Fig 2 and 3. to SI and provide the integrated OH exposure as additional time axis.

Reply: As suggested we have moved Fig 2 and 3 to SI, and provided the integrated OH exposure in Fig 3 (now Fig. S3) as follows:

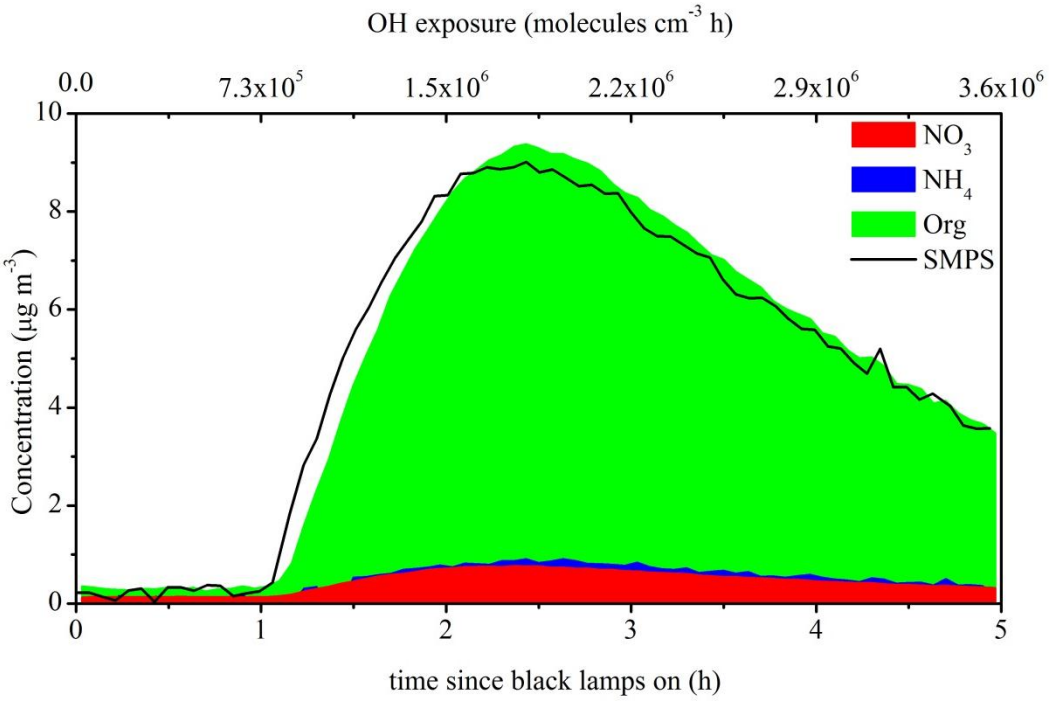

Q13- Section 2.4.2, please clarify how refractory particulate matter (elemental carbon) has been taken into account in the analysis, or discuss, why you assume that the vehicle exhaust studied in the smog chamber consist only of non-refractory material.

Reply: This question has been addressed in Q3.

Q14- Section 2.4.2, please clarify that the discrepancy between SMPS and AMS derived mass in the presented experiments also results from different size-dependent measurement cut-offs (you mention very small particle size of at least the primary particles, which are well below the optimum lens transmission of the AMS), and not only from AMS collection efficiency.

Reply: This question has been addressed in Q3.

Q15- Section 2.4.2, page 10562, line 12: please remove "the two", the sentence should read: "However, both methods have limitations".

Reply: revised as suggested.

Q16- Section 2.4.3, line 13 (page 10563), please specify "simulating air".

Reply: "simulating air" was changed to "*air samples*" in the revised manuscript.

Q17- For all data presented in Tables and Figures: where data are available, please add error bars to the data and indicate which kind of averaging method has been applied to the data of different experiments.

Reply: Uncertainties for temperature and relative humidity were presented in Table 2 in the revised manuscript. Error bars of NMHCs measurements were added to Fig. 4 (now Fig. 2 in the revised manuscript) as follows:

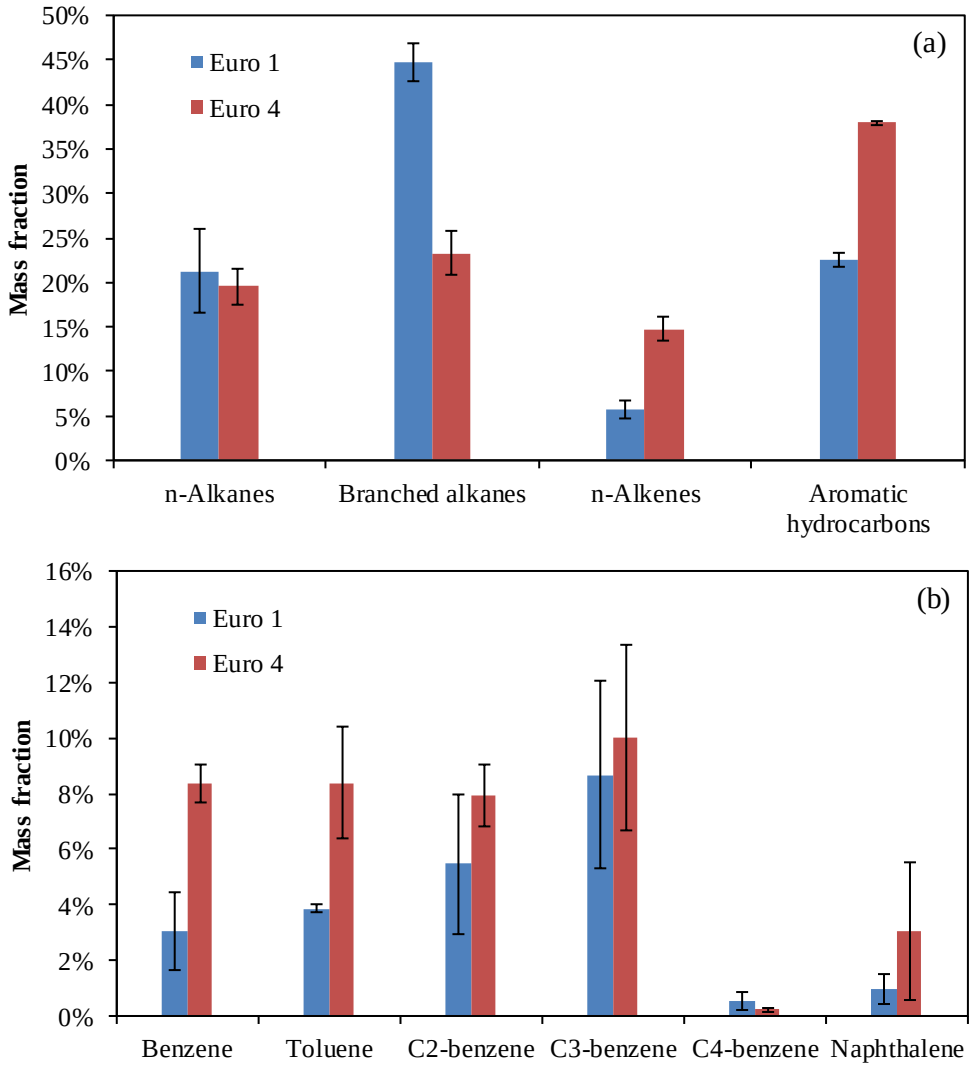

Q18- Please use either NMHC or VOC in the manuscript for purpose of consistency, and specify the measurement principle (GC-FID or GC-MSD or PTR-TOF-MS where needed, e.g. in Table 2, 3, 5, and Figure 4 and 5.

Reply: NMHCs were changed to "*VOCs*" throughout the revised manuscript. The

sentence “C2-C3 and C4-C12 hydrocarbons were measured by GC-FID and GC-MSD, respectively.” was added to the revised manuscript. The measurement principle has been specified.

Q19- Section 3.1, line 11-13 and line 18-19, please compare the results with Huang et al., 2015, ACPD (doi:10.5194/acpd-15-7977-2015), and other literature to narrow down whether fuel, vehicle type or emission standards are causing the difference in the two vehicles, or whether the difference lies within the statistical range. Previous publications have shown a wide spread in vehicle emissions for different vehicles and test conditions, and a comparison of 1 vehicle to another to conclude for a whole class of vehicles from one emission standard is not justified.

Reply: The discussion has been extended in the revised manuscript and also presented here.

Change “Aromatic hydrocarbons accounted for about…vehicle type and emission standard” to “Aromatic hydrocarbons accounted for about 38.0% and 22.5% of the total VOCs for Euro 4 and 1 vehicle, respectively, relatively higher than 10-15% observed by Nordin et al. (2013) for idling Euro 2, 3 and 4 vehicles. The mass fraction of aromatic hydrocarbons for Euro 4 vehicle was comparable with 32.2% for idling private cars in Hong Kong (Guo et al., 2011) and 38.3% for Euro 3 light-duty gasoline vehicles operated through ECE cycles with an average speed around 18.7 km h^{-1} (Wang et al., 2013). Both Schauer et al. (2002) and Gentner et al. (2013) observed that aromatic hydrocarbons contributed around 27% of the total VOCs for gasoline-powered automobiles driven through the cold-start Federal Test Procedure urban driving cycle and on-road gasoline vehicles in the Caldecott tunnel, similar with that of Euro 1 vehicle in this study. Recently, Huang et al. (2015) reported that mass fractions of aromatic hydrocarbons were as high as 46.4% for Euro 1, 2, and 3 light-duty gasoline vehicles operated through ECE cycles. Therefore, the variations of the composition of LDGV exhausts in this study were within the range of previous studies.”

Add “Using 7.87 L/100 km as the average fuel efficiency (Wagner et al., 2009), we obtained the VOCs emission factors based on g km^{-1} for Euro 4 and 1 vehicle to be

0.12 and 0.46 g km^{-1}, respectively, comparable with the previous reported values for Euro 1 and 4 gasoline vehicles in China (Huo et al., 2012; Huang et al., 2015). According to previous studies, there is a clear reduction of VOCs emissions from gasoline vehicles with stricter emission standards (Huo et al., 2012; Huang et al., 2015).” before “It is worth noting that…”

Q20- Section 3.1, the authors have used a PTR-TOF-MS in the course of the study. I suggest adding a comparison of GD-FID/MSD data with PTR-TOF-MS data to this section.

Reply: This question has been addressed in Q4.

Q21- Section 3.1, I suggest to include information in Table 5 into Figure 4, and remove Table 5 or provide in SI.

Reply: Additional information in Table 5 was added to Figure 4, now Fig. 2 in the revised manuscript, also shown in Q17.

Q22- Section 3.2, Fig 5ab: please provide also the integrated OH exposure as time axis in addition to the “time since lights on” in the Fig.

Reply: The integrated OH exposure was added as time axis to Fig 5ab (now Fig. 3ab).

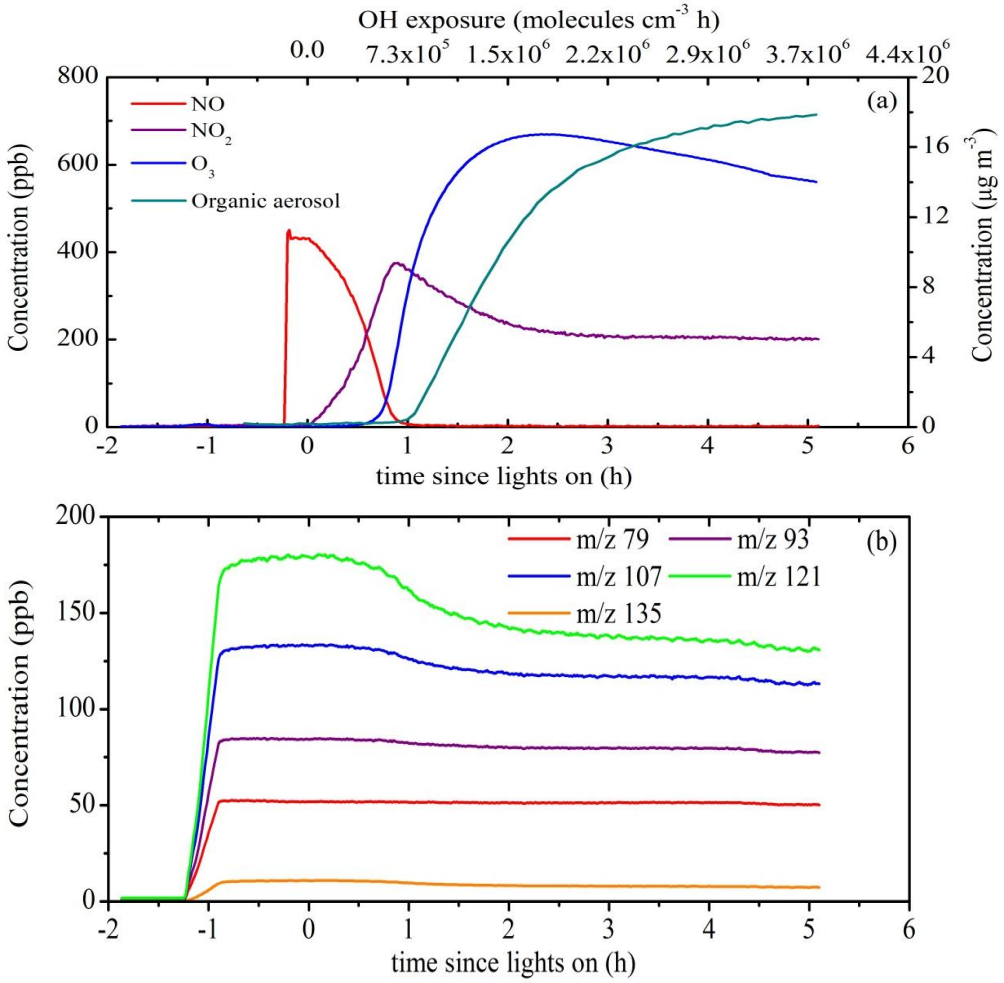

Q23-I suggest to discuss Fig. 5c and the statement in section 3.2, page 10565, line 11 – 14,“ As shown in Fig. 5c, the total particle number concentration increased fast from 82 to 116 143 cm^{-3} in approximately 10 min, indicating dramatic new particle formation. After nucleation occurred, the mean diameter increased from 20 to 60 nm in about 1.5 h” as a potential limitation of the study, rather than a result. Rather than this being a significant result of the investigations, the fact that nucleation occurs during these experiments points to experimental weakness of the study, which is, that no sufficient aerosol seed surface is provided. This can lead to significant losses of vapors to chamber walls, as demonstrated in recent publications (Zhang, et al., 2014). In addition, the small starting particle number concentration in the smog chamber (82 cm-3), points to significant losses during sampling into the smog chamber.

Reply: This question has been addressed in Q1 and Q2.

Q24- The statement in section 3.2, page 10565, line 14 – 17 “Because particles with diameters larger than 50 nm can act as cloud condensation nuclei (CCN) (Mc Figgans

et al., 2006) and influence the radiative forcing, SOA from vehicle exhausts may has climate effects to a certain extent as well as air quality effects." should be removed, unless the authors can provide experimental evidence.

Reply: This sentence has been removed in the revised manuscript.

Q25- Section 3.2, page 10565, please reformulate Line 18 to "SOA production factors (PF) for the LDGVs tested in this study" instead of "for LDGVs in China".

Reply: revised as suggested.

Q26-Section 3.2, page 10565, Line 25 onwards ("Decay of toluene . . ."): the section on estimation of OH exposure should be moved to "Materials and methods".

Reply: revised as suggested.

Q27- Section 3.3: Table 3 and Figure 7 present essentially the same information. Please include additional information provided in Table 3 into Figure 7 and remove Table 3 or provide Table 3 in SI.

Reply: Table 3 has been moved to SI.

Q28- Section 3.3: Table 4: please provide some extended discussion on why the yields observed in the smog chamber are around 3% for vehicle II and 10 – 20% for vehicle I. Please link the difference in the yield with the chemical composition of the precursor gases to find an explanation.

Reply: The discussion has been extended in the revised manuscript and also presented here.

"As shown in Table 3, SOA yields for Euro 1 vehicle were around 3%, quite lower than 10%-17% for Euro 4 vehicle. The mass fraction of aromatic hydrocarbons for Euro 4 vehicle was about two times higher than that for Euro 1 vehicle (Fig. 2a), which would form more semi-volatile organic compounds (SVOCs) partitioning into particle phase under similar OH exposure and thus lead to the relatively higher SOA yields."

Q29-Section 4, Conclusions: I recommend removing this section fully, as no real conclusions are drawn and a summary of the results and discussion section is superfluous.

Reply: This section has been removed as suggested.

References

Barletta, B., Meinardi, S., Sherwood Rowland, F., Chan, C.-Y., Wang, X., Zou, S., Yin Chan, L., and Blake, D. R.: Volatile organic compounds in 43 Chinese cities, Atmos Environ. 2005, 39, 5979-5990.

Cocker Iii, D. R., Mader, B. T., Kalberer, M., Flagan, R. C., and Seinfeld, J. H.: The effect of water on gas–particle partitioning of secondary organic aerosol: II. m-xylene and 1,3,5-trimethylbenzene photooxidation systems, Atmos. Environ. 2001, 35, 6073-6085.

Gentner, D. R., Worton, D. R., Isaacman, G., Davis, L. C., Dallmann, T. R., Wood, E. C., Herndon, S. C., Goldstein, A. H., and Harley, R. A.: Chemical Composition of Gas-Phase Organic Carbon Emissions from Motor Vehicles and Implications for Ozone Production, Environ. Sci. Technol. 2013, 47, 11837-11848.

Gormley, P. G., and Kennedy, M.: Diffusion from a Stream Flowing through a Cylindrical Tube, Proceedings of the Royal Irish Academy. Section A: Mathematical and Physical Sciences.1949, 52, 163-169.

Guo, H., Zou, S. C., Tsai, W. Y., Chan, L. Y., and Blake, D. R.: Emission characteristics of nonmethane hydrocarbons from private cars and taxis at different driving speeds in Hong Kong, Atmos. Environ. 2011, 45, 2711-2721.

Huang, C., Wang, H. L., Li, L., Wang, Q., Lu, Q., de Gouw, J. A., Zhou, M., Jing, S. A., Lu, J., and Chen, C. H.: VOC species and emission inventory from vehicles and their SOA formation potentials estimation in Shanghai, China, Atmos. Chem. Phys. Discuss. 2015, 15, 7977-8015.

Huo, H., Yao, Z., Zhang, Y., Shen, X., Zhang, Q., Ding, Y., and He, K.: On-board measurements of emissions from light-duty gasoline vehicles in three mega-cities of China, Atmos. Environ. 2012, 49, 371-3772012.

Liu, P. S. K., Deng, R., Smith, K. A., Williams, L. R., Jayne, J. T., Canagaratna, M. R., Moore, K., Onasch, T. B., Worsnop, D. R., and Deshler, T.: Transmission Efficiency of an Aerodynamic Focusing Lens System: Comparison of Model Calculations and Laboratory Measurements for the Aerodyne Aerosol Mass Spectrometer, Aerosol.

Sci. Tech. 2007, 41, 721-733.

Wagner, D. V., An, F., and Wang, C.: Structure and impacts of fuel economy standards for passenger cars in China, Energy. Policy. 2009, 37, 3803-3811.

Wang, J., Jin, L., Gao, J., Shi, J., Zhao, Y., Liu, S., Jin, T., Bai, Z., and Wu, C.-Y.: Investigation of speciated VOC in gasoline vehicular exhaust under ECE and EUDC test cycles, Sci. Total Environ. 2013, 445–446, 110-116.

Wehner, B., Wiedensohler, A., Tuch, T. M., Wu, Z. J., Hu, M., Slanina, J., and Kiang, C. S.: Variability of the aerosol number size distribution in Beijing, China: New particle formation, dust storms, and high continental background, Geophys. Res. Lett. 2004, 31, L22108.

Zhang, X., Cappa, C. D., Jathar, S. H., McVay, R. C., Ensberg, J. J., Kleeman, M. J., and Seinfeld, J. H.: Influence of vapor wall loss in laboratory chambers on yields of secondary organic aerosol, Proceedings of the National Academy of Sciences. 2014.

Zhang, X., Schwantes, R. H., McVay, R. C., Lignell, H., Coggon, M. M., Flagan, R. C., and Seinfeld, J. H.: Vapor wall deposition in Teflon chambers, Atmos. Chem. Phys. 2015, 15, 4197-4214.

A list of relevant changes

Line 28 –Delete "However, there are still no…SOA formation from vehicle exhausts"

Line 31–Add "operated" after "and Euro 4)"

Line 36–Change "the quite similar" to "comparable"

Line 40–Change "form" to "from"

Line 94-95–Change "However, in China…The possession of LDGVs was 98.8 million in 2012 in China…" to "In China, the number of LDGVs reached 98.8 million in 2012 and increased…"

Line 40–Change "Zhang et al., 2015" to "Y. L. Zhang et al., 2015"

Line 107–Add "operated" after "(LDGVs)"

Line 138–Change "NMHCs" to "VOCs"

Line 148 –Delete "/electron capture detector" and "/ECD"

Line 150-154–Add "C2-C3 and C4-C12 hydrocarbons were measured by GC-FID and GC-MSD, respectively. In this study, the offline measurement was the standard method to determine the mass concentrations of VOCs. PTR-TOF-MS was used for deriving the time-resolved concentrations of VOCs." after "…Y. L. Zhang et al., 2010, 2012, 2013)."

Line 180-182–Add "Conductive silicon tubes were used as sampling lines for HR-TOF-MS and SMPS to reduce electrostatic losses of particles." after "…(Zhang et al., 2005)."

Line 201-202–Change "VOCs in these samples…mentioned above" to "VOCs and CO_2 in these samples were measured offline by the same methods mentioned above to characterize the primary emissions from the exhaust pipe"

Line 211-230–Add "Blank experiments with no vehicle exhaust introduced were performed to quantify the reactivity of the matrix gas. After 5 h of irradiation, the number and mass of formed particles were <5 cm^{-3} and 0.1 μg m^{-3}, respectively.
During the introduction of exhausts, particles and VOCs might deposit to the surface of the transfer lines. Therefore, a flow rate of as high as 20 L min^{-1} and a transfer line of as short as 5 m were used to provide residence time within seconds, and thus reduce the losses of particles and VOCs in the transfer lines. Furthermore, before being introduced into the reactor, exhausts were generally pumped through the

transfer lines for half an hour to saturate the transfer lines with particles and VOCs while warming the catalytic converter. Losses of particles and VOCs in the introduction lines were determined by comparing the concentrations of total particle number and VOCs in the directly emitted exhausts with the ones after passing through the transfer lines. The loss of total particle number was estimated to be less than 3%. The penetration efficiency of particles due to diffusion in a cylindrical tube, η(dp), can be also estimated by a laminar diffusional deposition model (Gormley and Kennedy, 1949). For particles with diameters larger than 10 nm, the penetration efficiency was higher than 95%, indicating minor losses of particles in the transfer line. The losses of VOCs in the transfer line were estimated to be less than 5%, which might lead to a small underestimation of SOA production." after "…3 h to correct the particles wall loss."

Line 245–Change "Fig. 2" to "Fig. S1 in the Supplement"

Line 257 –Delete "the two"

Line 263–Add "the transmission efficiency (Liu et al., 2007) and" after "…mass due to"

Line 265-272–Add "Fig. S2 shows the particle volume distribution measured by SMPS for a typical smog chamber experiment (experiment 2). Most particles were in the range 40-120 nm after SOA formation. Since the transmission window of the standard lens of HR-TOF-AMS is 60-600 nm (aerodynamic diameter) (Liu et al., 2007), particles with diameter lower than 40 nm (mobility diameter) were cut from the lower edge of the volume distribution. After 1 h since nucleation occurred, only <5% of the mass was outside the transmission window of HR-TOF-MS, indicating that HR-TOF-AMS might underestimate the PM in the early stage of SOA formation." after "…and SMPS data."

Line 275–Change "Fig. 3" to "Fig. S3"

Line 282-284–Add "As shown in Fig. S3, the mass of primary particles measured by SMPS was comparable with that measured by HR-TOF-AMS, thus we assumed that the mass of black carbon (BC) in the reactor was negligible." after "…measured by the AMS."

Line 294-297–Change "…compounds is presented in Table 3…reacted organic precuresors" to "compounds is presented in Table S2. At the beginning and end of each experiment, air samples in the reactor were collected into 2 L electropolished and evacuated stainless steel canisters and analyzed by GC-MSD to determine the mass of reacted organic precursors."

Line 305-321–Add section 2.4.5 "Determination of OH exposure""" Decay of toluene

measured by PTR-TOF-MS is used to derive the average OH concentration during each experiment. Changes in the toluene concentration over time can be expressed as:

$$\frac{d[toluene]}{dt} = -k \cdot [OH] \cdot [toluene] \quad (3)$$

where k is the rate constant for the reaction between toluene and OH radical. Assuming a constant OH concentration during an experiment, we can integrate Eq. (3) to get Eq. (4):

$$\ln(\frac{[toluene]_0}{[toluene]_t}) = k \cdot [OH] \cdot t \quad (4)$$

So by plotting $ln([toluene]_0/[toluene]_t)$ versus time t, we can obtain a slope that equals $k \times [OH]$. The average OH concentration is therefore calculated as:

$$[OH] = \frac{slope}{k} \quad (5)$$

The OH exposure is then determined through multiplying the average OH concentration by time."

Line 324–Change "Fig. 4" to "Fig. 2"

Line 325–Change "vehicle I and II" to "Euro 4 and 1 vehicle"; Change "shared" to "contributed"

Line 326–Change "NMHCs" to "VOCs"

Line 327–Change "NMHCs" to "speciated VOCs"

Line 330–Change "NMHCs" to "VOCs"; Change "vehicle II" to "Euro 1 vehicle"; Change "vehicle I" to "Euro 4 vehicle"

Line 332–Change "NMHCs for vehicle I and II" to "VOCs for Euro 4 and 1 vehicle"

Line 333–Add "idling" after "…for"

Line 333-343–Add "The mass fraction of aromatic hydrocarbons for Euro 4 vehicle was comparable with 32.2% for idling private cars in Hong Kong (Guo et al., 2011) and 38.3% for Euro 3 light-duty gasoline vehicles operated through ECE cycles with an average speed around 18.7 km h^{-1} (Wang et al., 2013). Both Schauer et al. (2002) and Gentner et al. (2013) observed that aromatic hydrocarbons contributed around 27% of the total VOCs for gasoline-powered automobiles driven through the cold-start Federal Test Procedure urban driving cycle and on-road gasoline vehicles in the Caldecott tunnel, similar with that of Euro 1 vehicle. Recently, Huang et al. (2015) reported that mass fractions of aromatic hydrocarbons were as high as 46.4% for Euro

1, 2, and 3 light-duty gasoline vehicles operated through ECE cycles." after "…Euro 2, 3 and 4 vehicles."

Line 343-345–Change "The variations …emission standard" to "Therefore, the variations of the composition of LDGV exhausts in this study were within the range of previous studies."

Line 346–Change "NMHCs" to "VOCs"

Line 347–Change "vehicle I" to "Euro 4 vehicle"

Line 347-348–Change "1.3 and 0.5 times lower…vehicle II" to "26.0% and 43.5% of those for Euro 1 vehicle"

Line 350–Change " NMHCs for vehicle I" to "VOCs for Euro 4 vehicle"

Line 351-354–Add "Using 7.87 L/100 km as the average fuel efficiency (Wagner et al., 2009), we obtained the VOCs emission factors based on g km^{-1} for Euro 4 and 1 vehicles to be 0.12 and 0.46 g km^{-1}, respectively, comparable with the previous reported values for Euro 1 and 4 gasoline vehicles in China (Huo et al., 2012; Huang et al., 2015)." after "…(Platt et al., 2013)."

Line 355-356–Change "There is a clear reduction…stricter emission standards" to "According to previous studies, there is a clear reduction of VOCs emissions from gasoline vehicles with stricter emission standards (Huo et al., 2012; Huang et al., 2015)."

Line 360-363–Add "It is important to note that the reported data are only based on five chamber experiments with two LDGVs under idling conditions. More tests are needed to assess SOA formation from gasoline vehicle exhausts in China." after "…(Tong et al., 2000)."

Line 365–Change "Fig. 5" to "Fig. 3"

Line 374–Change "Table 4" to "Table 3"

Line 378–Change "Fig. 5c" to "Fig. 3c"

Line 379–Delete "in approximately 10 min"

Line 380-404–Change "After nucleation occurred…as well as air quality effects" to "…new particle formation, which might be due to that the starting surface concentrations of particles were all below a critical value (100–2000 μm^2 cm^{-3}, Table S1) (Wehner et al., 2004). As shown in Table S1, primary particle numbers in the

reactor in this study ranged from 82 to 18948 cm^{-3}, 1-2 orders of magnitude higher than that of a Euro 2 car operated at idling with a similar dilution ratio (Nordin et al., 2013), indicating that the small starting particle number concentrations might mainly due to the idling condition of tested cars rather than the losses in the introduction lines. In addition, upon entering into the chamber, emitted particles would partition due to dilution similar as in the atmosphere, regardless of the temperature and concentration in the sampling system, which might lead to the decrease of starting number concentrations. A certain extent of primary particles under the detection limit of 14 nm of SMPS also contributed to the measured small starting number concentration of particles.

Deposition of SOA-forming vapors to the walls might lead to the underestimation of SOA production. The wall loss rate coefficient of vapors is related with the numbers of carbon and oxygen in the molecule (X. Zhang et al., 2015). Here, we take $C_7H_8O_4$, a product of the photo-oxidation of toluene as an example. The loss of $C_7H_8O_4$ to walls would be 7% in an hour before SOA formation when a wall deposition rate of 2×10^{-5} s^{-1} was used (X. Zhang et al., 2015). After SOA formation, the surface concentrations of particles increased fast to as high as 2000 μm^2 cm^{-3} in an hour, which would reduce the vapor wall losses."

Line 405–Change "LDGVs in China" to "the LDGVs tested in this study"

Line 413-424–Delete "Decay of toluene measured by PTR-TOF-MS… $[OH] = \frac{slope}{k}$ (5)"

Line 425–Change "Table 4" to "Table 3"

Line 439-444–Add "As shown in Table 3, SOA yields for Euro 1 vehicle were around 3%, quite lower than 10%-17% for Euro 4 vehicle. The mass fraction of aromatic hydrocarbons for Euro 4 vehicle was about two times higher than that for Euro 1 vehicle (Fig. 2a), which would form more semi-volatile organic compounds (SVOCs) partitioning into particle phase under similar OH exposure and thus lead to the relatively higher SOA yields." after "…mass concentration of organic material."

Line 446–Change "Fig. 6" to "Fig. 4"

Line 449-473–Change "Compared with the study of Nordin…result in higher SOA yields" to "The effective SOA yields in the study of Nordin et al. (2013) were 60%-360% higher than those in this study at same concentrations of M_0. In their calculation of the reacted SOA precursors, C4-benzene and naphthalene were excluded. The effective SOA yields would increase 7%-34% when C4-benzene and naphthalene were excluded in this study, which could explain a small portion of the discrepancy. According to the estimation above, the loss of VOCs in the transfer lines

was less than 5%. A little higher than VOCs, if assumed to be 20%, losses of IVOCs and SVOCs in the transfer lines would increase the SOA effective yields by a factor of 2%-10% when the unexplained SOA discussed later was all attributed to the contribution from IVOCs and SVOCs. The existence of seed particles in the study of Nordin et al. (2013) might reduce the wall loss of semi-volatile organic vapors and thus increase the effective SOA yield (Kroll et al., 2007; Zhang et al., 2014; X. Zhang et al., 2015). However, Cocker et al. (2001) found that SOA formation from m-xylene and 1,3,5-trimethylbenzene photo-oxidation was unaffected by the presence of ammonium sulfate seed aerosols. The influence of seed particles on SOA yields still needs further investigations. Faster oxidation rates caused by higher OH concentrations in the study of Nordin et al. (2013) would also result in higher SOA yields (Ng et al., 2007)."

Line 483-489–Add "SOA yield curves of toluene and m-xylene from Ng et al. (2007) were also widely used to estimate SOA production (Platt et al., 2013). However, the introduction of seed aerosols and OH precursor made the SOA yield curves in the study of Ng et al. (2007) not suitable for this study. Considering that the study of Odum et al. (1997) provided a systematic estimation of SOA yields from toluene, C2-benzene, C3-benzene and C4-benzene, we mainly used the two-product curves from Odum et al. (1997) to estimate the SOA production." after "…Shakya et al. (2010)."

Line 493–Change "Table 3" to "Table S2"

Line 494–Change "Fig. 7" to "Fig. 5"

Line 498–Change "Table 5" to "Fig. 2b"

Line 499–Change "NMHCs" to "VOCs"

Line 514–Change "intermediate-volatility organic compounds (IVOCs)" to "IVOCs"

Line 525-528–Add "Wall losses of organic vapors were not considered in this study, which would lead to the underestimation of SOA production. Therefore, the mass closure analysis estimated the maximum amount of SOA that could be explained by aromatics." after "…(Song et al., 2007)."

Line 541–Change "Fig. 8a" to "Fig. 6a"

Line 561–Change "Fig. 8b" to "Fig. 6b"

Line 574-586–Delete the section "Conclusion"

Line 623–Add the reference "Cocker Iii, D. R., Mader, B. T., Kalberer, M., Flagan, R.

C., and Seinfeld, J. H.: The effect of water on gas–particle partitioning of secondary organic aerosol: II. m-xylene and 1,3,5-trimethylbenzene photooxidation systems, Atmos Environ, 35, 6073-6085, http://dx.doi.org/10.1016/S1352-2310(01)00405-8, 2001."

Line 649–Add the reference "Gentner, D. R., Worton, D. R., Isaacman, G., Davis, L. C., Dallmann, T. R., Wood, E. C., Herndon, S. C., Goldstein, A. H., and Harley, R. A.: Chemical Composition of Gas-Phase Organic Carbon Emissions from Motor Vehicles and Implications for Ozone Production, Environ. Sci. Technol., 47, 11837-11848, doi:10.1021/es401470e, 2013."

Line 659–Add references "Gormley, P. G., and Kennedy, M.: Diffusion from a Stream Flowing through a Cylindrical Tube, Proceedings of the Royal Irish Academy. Section A: Mathematical and Physical Sciences, 52, 163-169, doi:10.2307/20488498, 1949.
Guo, H., Zou, S. C., Tsai, W. Y., Chan, L. Y., and Blake, D. R.: Emission characteristics of nonmethane hydrocarbons from private cars and taxis at different driving speeds in Hong Kong, Atmos. Environ., 45, 2711-2721, http://dx.doi.org/10.1016/j.atmosenv.2011.02.053, 2011."

Line 704–Add references "Huang, C., Wang, H. L., Li, L., Wang, Q., Lu, Q., de Gouw, J. A., Zhou, M., Jing, S. A., Lu, J., and Chen, C. H.: VOC species and emission inventory from vehicles and their SOA formation potentials estimation in Shanghai, China, Atmos. Chem. Phys. Discuss., 15, 7977-8015, 10.5194/acpd-15-7977-2015, 2015.
Huo, H., Yao, Z., Zhang, Y., Shen, X., Zhang, Q., Ding, Y., and He, K.: On-board measurements of emissions from light-duty gasoline vehicles in three mega-cities of China, Atmos. Environ., 49, 371-377, doi:10.1016/j.atmosenv.2011.11.005, 2012."

Line 769–Add references "Liu, P. S. K., Deng, R., Smith, K. A., Williams, L. R., Jayne, J. T., Canagaratna, M. R., Moore, K., Onasch, T. B., Worsnop, D. R., and Deshler, T.: Transmission Efficiency of an Aerodynamic Focusing Lens System: Comparison of Model Calculations and Laboratory Measurements for the Aerodyne Aerosol Mass Spectrometer, Aerosol. Sci. Tech., 41, 721-733, 10.1080/02786820701422278, 2007.
Liu, T. Y., Wang, X. M., Wang, B. G., Ding, X., Deng, W., Lü, S. J., and Zhang, Y. L.: Emission factor of ammonia (NH_3) from on-road vehicles in China: tunnel tests in urban Guangzhou, Environ. Res. Lett., 9, 064027, 2014."

Line 777–Delete the reference "Lu, Z…2009"

Line 875–Add references "Wagner, D. V., An, F., and Wang, C.: Structure and impacts of fuel economy standards for passenger cars in China, Energy. Policy., 37, 3803-3811, doi:10.1016/j.enpol.2009.07.009, 2009.
Wang, J., Jin, L., Gao, J., Shi, J., Zhao, Y., Liu, S., Jin, T., Bai, Z., and Wu, C.-Y.:

Investigation of speciated VOC in gasoline vehicular exhaust under ECE and EUDC test cycles, Sci. Total Environ., 445–446, 110-116, http://dx.doi.org/10.1016/j.scitotenv.2012.12.044, 2013."

Line 892–Add the reference "Wehner, B., Wiedensohler, A., Tuch, T. M., Wu, Z. J., Hu, M., Slanina, J., and Kiang, C. S.: Variability of the aerosol number size distribution in Beijing, China: New particle formation, dust storms, and high continental background, Geophys. Res. Lett., 31, L22108, 10.1029/2004GL021596, 2004."

Line 921–Add references "Zhang, X., Cappa, C. D., Jathar, S. H., McVay, R. C., Ensberg, J. J., Kleeman, M. J., and Seinfeld, J. H.: Influence of vapor wall loss in laboratory chambers on yields of secondary organic aerosol, Proceedings of the National Academy of Sciences, 10.1073/pnas.1404727111, 2014.
Zhang, X., Schwantes, R. H., McVay, R. C., Lignell, H., Coggon, M. M., Flagan, R. C., and Seinfeld, J. H.: Vapor wall deposition in Teflon chambers, Atmos. Chem. Phys., 15, 4197-4214, 10.5194/acp-15-4197-2015, 2015."

Table 2. Initial conditions for the light-duty gasoline vehicle photooxidation experiments.

Experiment #	Vehicle ID	T (℃)[a]	RH (%)[a]	VOC/ NO_x	VOCs (ppbv)[b]	NO (ppbv)	NO_2 (ppbv)
1	Ⅰ	25.8±0.7	52.0±1.8	10.2	1368	115.1	18.4
2	II	24.1±0.6	57.0±2.0	6.0	2583	431.0	0.6
3	Ⅰ	25.0±0.8	52.9±2.0	9.3	2896	300.6	9.5
4	Ⅰ	24.2±0.8	52.5±2.7	2.0	1885	794.1	161.9
5	II	25.0±0.3	52.6±1.3	7.2	1507	210.4	0.7

[a]: Stated uncertainties (1σ) are from scatter in temperature and relative humidity, respectively.

[b]: C2-C3 and C4-C12 hydrocarbons were measured by GC-FID and GC-MSD, respectively.

Table 3 was moved to the supplement as **Table S2**.

Table 5 was removed.

Fig. 2 and 3 was moved to the supplement as **Fig. S1 and S3**.

Fig. 4 was revised, now presented as **Fig. 2**.

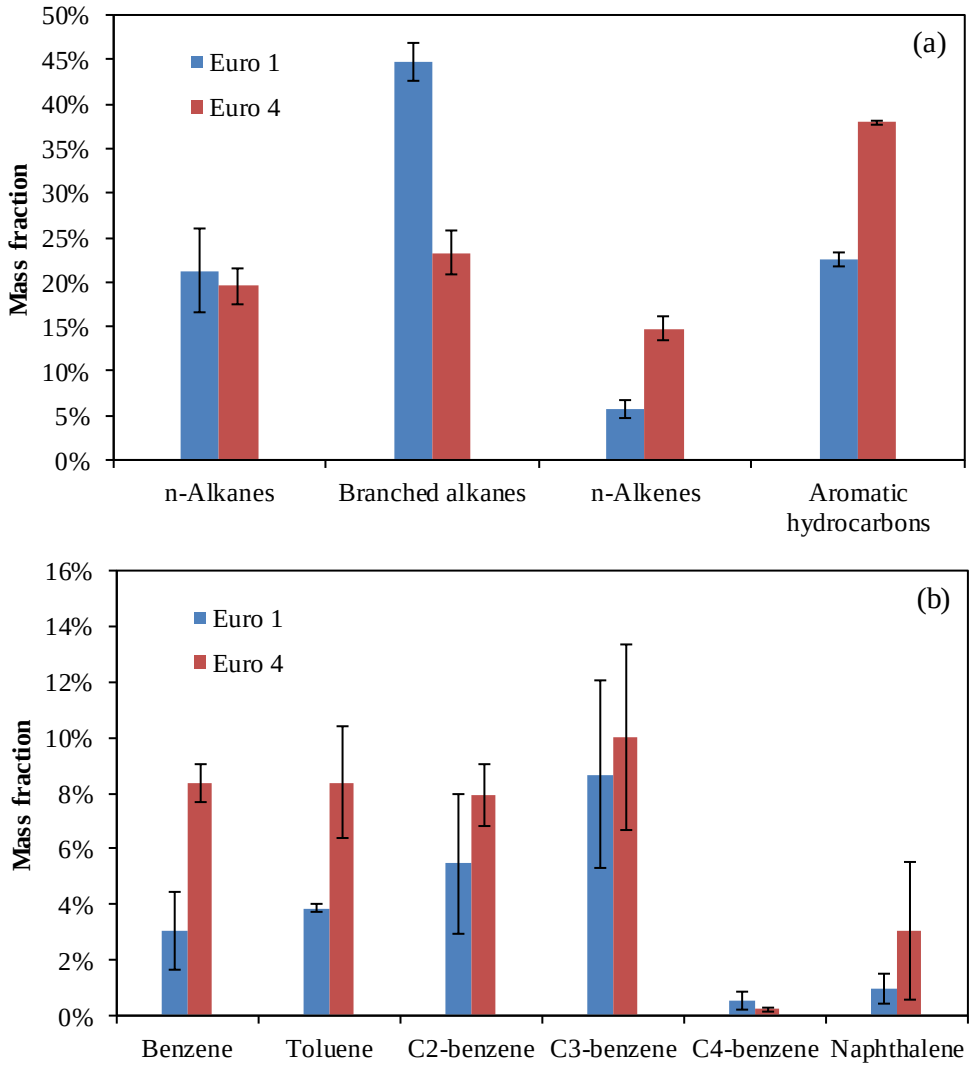

Fig. 2. Composition of **(a)** VOCs and **(b)** aromatics of gasoline vehicle exhausts from Euro 1 and Euro 4 private cars, presented as weight percentage of speciated VOCs. C2-C3 and C4-C12 hydrocarbons were measured by GC-FID and GC-MSD, respectively. The error bars (1σ) represent variability from measurements for each vehicle.

Fig. 5 was revised, now presented as **Fig. 3**.

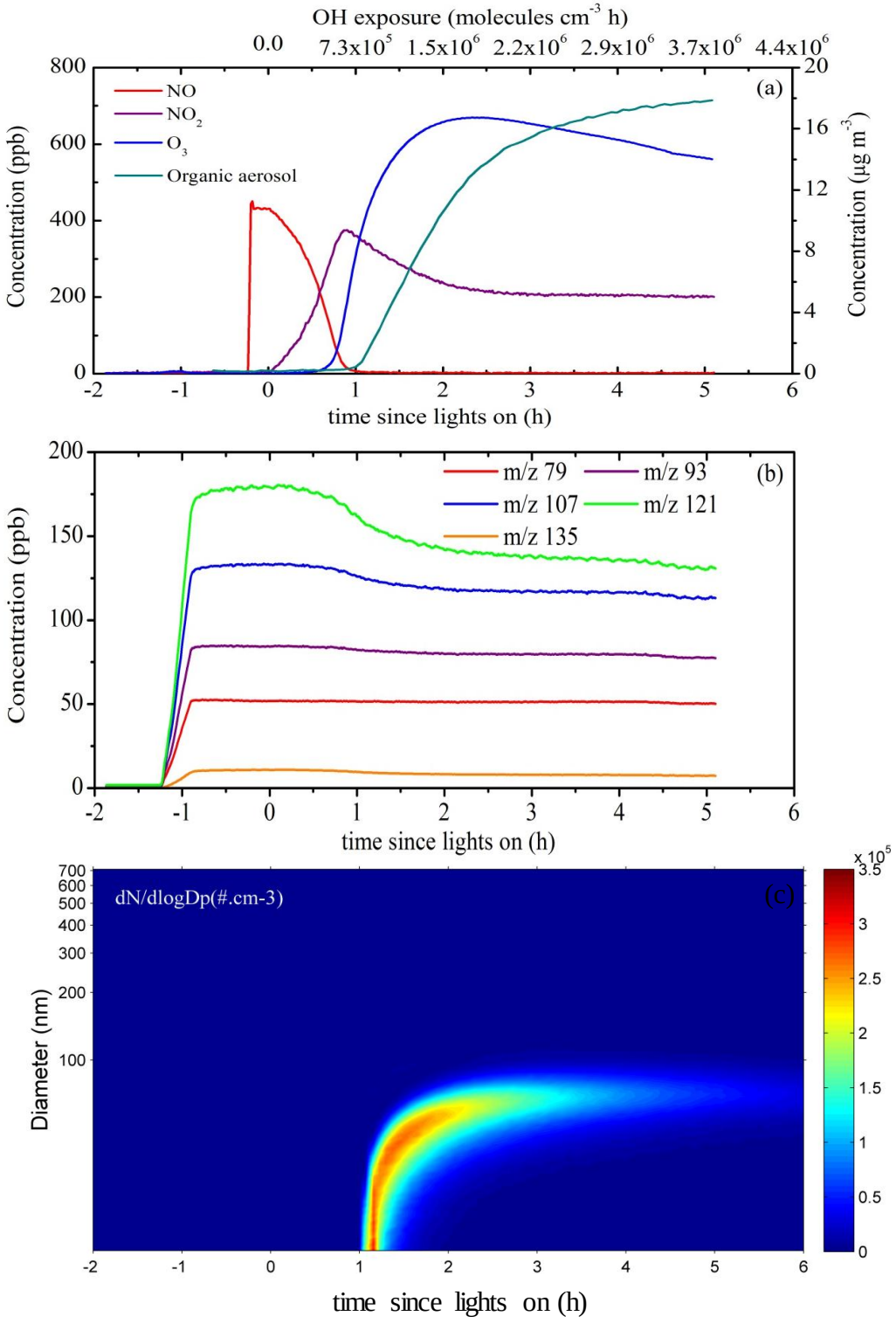

Fig. 3. Concentration–time plots of gas–phase and particle–phase species and particle number concentration distribution as a function of time during a typical smog chamber experiment (experiment 2): **(a)** NO, NO_2, O_3 (left *y* axis) and organic aerosol (right *y* axis); **(b)** gas-phase light aromatics (measured by PTR-TOF-MS) (benzene characterized by m/z 79; toluene characterized by m/z 93; C_2–benzene characterized

by m/z 107; C_3–benzene characterized by m/z 121; C_4-benzene characterized by m/z 135); **(c)** particle size-number concentration distributions as a function of time. The vehicle exhaust was introduced into the reactor between -1.3 h and -0.85 h; the primary emissions were characterized from -0.85 h to 0 h; at time = 0 h, the black lamps were turned on.

The caption of **Fig. 6** was revised, now presented as **Fig. 4**.

Fig. 4. Comparison of yield data obtained for the gasoline experiments in this study with that of Nordin et al. (2013). The green line is the best fit one-product model (α_1 = 0.311, $K_{om,1}$ = 0.043) for the data set of Nordin et al. (2013). The orange line is the best one-product fit to the effective SOA yield in this study (α_1 = 0.350, $K_{om,1}$ = 0.007). Organic precursors in the calculation of effective yields included benzene, toluene, C2–benzene, C3–benzene, C4-benzene and naphthalene.

Fig. 7 was now presented as **Fig. 5**.

Fig. 8 was now presented as **Fig. 6**.

Secondary organic aerosol formation from photochemical aging of light-duty gasoline vehicle exhausts in a smog chamber

Tengyu Liu[1,2], Xinming Wang[1,3,*], Wei Deng[1,2], Qihou Hu[1], Xiang Ding[1], Yanli Zhang[1], Quanfu He[1,2], Zhou Zhang[1,2], Sujun Lü[1,2], Xinhui Bi[1], Jianmin Chen[4], Jianzhen Yu[5]

1. State Key Laboratory of Organic Geochemistry, Guangzhou Institute of Geochemistry, Chinese Academy of Sciences, Guangzhou 510640, China
2. University of Chinese Academy of Sciences, Beijing 100049, China
3. Guangdong Key Laboratory of Environmental Protection and Resources Utilization, Guangzhou Institute of Geochemistry, Chinese Academy of Sciences, Guangzhou 510640, China
4. Shanghai Key Laboratory of Atmospheric Particle Pollution and Prevention, Department of Environmental Science & Engineering, Fudan University, Shanghai 200433, China
5. Division of Environment, Hong Kong University of Science & Technology, Clear Water Bay, Kowloon, Hong Kong, China

*Corresponding author:

Dr. Xinming Wang

State Key Laboratory of Organic Geochemistry

Guangzhou Institute of Geochemistry, Chinese Academy of Sciences

Tel: +86-20-85290180; Fax: +86-20-85290706

Email: wangxm@gig.ac.cn

Abstract

In China, fast increase in passenger vehicles has procured the growing concern about vehicle exhausts as an important source of anthropogenic secondary organic aerosols (SOA) in megacities hard-hit by haze. ~~However, there are still no chamber simulation studies in China on SOA formation from vehicle exhausts.~~ In this study, the SOA formation of emissions from two idling light-duty gasoline vehicles (LDGVs) (Euro 1 and Euro 4) operated in China was investigated in a 30 m^3 smog chamber. Five photo-oxidation experiments were carried out at 25 ℃ with the relative humidity around 50%. After aging at an OH exposure of 5×10^6 molecules cm^{-3} h, the formed SOA was 12–259 times as high as primary OA (POA). The SOA production factors (PF) were 0.001–0.044 g kg^{-1} fuel, comparable with those from the previous studies at ~~the quite similar~~comparable OH exposure. This quite lower OH exposure than that in typical atmospheric condition might however lead to the underestimation of the SOA formation potential from LDGVs. Effective SOA yield data in this study were well fit by a one-product gas-particle partitioning model and quite lower than those of a previous study investigating SOA formation ~~form~~ from three idling passenger vehicles (Euro 2–Euro 4). Traditional single-ring aromatic precursors and naphthalene could explain 51%–90% of the formed SOA. Unspeciated species such as branched and cyclic alkanes might be the possible precursors for the unexplained SOA. A high-resolution time-of-flight aerosol mass spectrometer was used to characterize the chemical composition of SOA. The relationship between f_{43} (ratio of m/z 43, mostly

$C_2H_3O^+$, to the total signal in mass spectrum) and f_{44} (mostly CO_2^+) of the gasoline vehicle exhaust SOA is similar to the ambient semi-volatile oxygenated organic aerosol (SV-OOA). We plot the O:C and H:C molar ratios of SOA in a Van Krevelen diagram. The slopes of ΔH:C/ΔO:C ranged from -0.59 to -0.36, suggesting that the oxidation chemistry in these experiments was a combination of carboxylic acid and alcohol/peroxide formation.

1. Introduction

The formation mechanisms, magnitude and chemical composition of airborne fine particulate matter ($PM_{2.5}$) are important to evaluate its effects on human health and climate (Hallquist et al., 2009). Organic aerosol (OA) contributes roughly ~20% – 50% of the total fine particle mass at continental mid-latitudes (Saxena and Hildemann, 1996; Kanakidou et al., 2005). Atmospheric OA includes primary organic aerosol (POA) emitted from sources such as combustion of fossil fuels, biomass burning and volcanic eruptions, and secondary organic aerosol (SOA) formed via gas-particle conversion such as nucleation, condensation, and heterogeneous and multiphase chemistry or the aging of POA (Donahue et al., 2009; Jimenez et al., 2009). SOA is ubiquitous and dominates the total OA in various atmospheric environments, accounting for approximately two-thirds of the total OA in urban areas to almost 90% in urban downwind and rural areas in Northern Hemisphere mid-latitudes (Zhang et al., 2007). China, for example, has serious air quality problem due to $PM_{2.5}$ pollution in the recent decade (Chan and Yao 2008, Q. Zhang et al 2012), and SOA had contributed 30% – 90% of OA mass in its megacities (He et al., 2001; Cao et al., 2003; Duan et al., 2005, 2007; Yang et al., 2005; Hagler et al., 2006). However, models generally underestimate the observed OA levels mainly due to the unclear sources and formation processes of SOA (de Gouw et al., 2005; Heald et al., 2005; Johnson et al., 2006; Volkamer et al., 2006).

Vehicle exhausts emit plenty of primary PM and volatile organic compounds

(VOCs) containing precursors of SOA, influencing the near-surface atmospheric chemistry and the air quality, especially in urban areas. SOA formation from diesel generators and vehicles has been widely studied in smog chambers, demonstrating that the SOA mass formed from the exhaust of diesel generators and medium-, and heavy-duty diesel vehicles (HDDVs) usually exceeds the mass of emitted POA (Robinson et al., 2007; Weitkamp et al., 2007; Chirico et al., 2010; Miracolo et al., 2010; Samy and Zielinska, 2010; Nakao et al., 2011; Kroll et al., 2012). However, there are few studies on the SOA formation from gasoline vehicle exhausts. Nordin et al. (2013) investigated SOA formation from idling gasoline exhausts from three passenger vehicles (Euro 2 – Euro 4), finding that C_6-C_9 light aromatics contributed up to 60% of the formed SOA. While Platt et al. (2013) estimated aromatic precursors including C_6-C_{10} light aromatics and naphthalene were responsible for less than 20% of the SOA formed from the aging of emissions from a Euro 5 gasoline car operated during a New European Driving Cycle. To exclude the influence of a small sample size, Gordon et al. (2014) studied aging of emissions from 15 light-duty gasoline vehicles with model years ranging from 1987 to 2011, concluding that traditional precursors could fully explain the SOA from oldest vehicles and unspeciated organics were responsible for the majority of the SOA from the newer vehicles. Therefore, chemical compositions of SOA formed from gasoline vehicle exhaust varied a lot among vehicles with different types, model years and operating conditions.

~~However, in China there is still no information on SOA formation from vehicle~~

exhausts in the literature. In China, tThe possession number of LDGVs was reached 98.8 million in 2012 in China and increased at a rate of approximately 20% per year since 2005 (NBSC, 2013). Furthermore, gasoline fuel in China has relatively higher mass content of alkenes and aromatic hydrocarbons than that in US (Schauer et al., 2002; Zhang et al., 2013), and current emission standards of LDGVs in China lag behind European countries and US. The emission factors of $PM_{2.5}$, organic carbon (OC), element carbon (EC), NO_x, SO_2, NH_3 and non-methane hydrocarbons (NMHCs) for on-road vehicles in China were quite different from those in other countries (Liu et al., 2014; Y. L. Zhang et al., 2015). Therefore, it is urgent to investigate the SOA formation from vehicle exhaust in China to help make suitable policies to mitigate air pollution and also to provide valuable parameters to chemical transport models.

Here, we directly introduced dilute emissions from two idling light-duty gasoline vehicles (LDGVs) operated in China to a smog chamber to investigate the SOA formation. The magnitude and composition of the SOA formed from gasoline vehicle exhaust and whether traditional SOA precursors can explain the formed SOA was evaluated and discussed in this paper.

2. Materials and methods

2.1 Experimental setup

The photochemical aging experiments were carried out in the smog chamber in Guangzhou Institute of Geochemistry, Chinese Academy of Sciences (GIG-CAS). The GIG-CAS smog chamber has a 30 m^3 fluorinated ethylene propylene (FEP) reactor

116 housed in a temperature-controlled room. Details of setup and facilities about the
117 chamber have been described elsewhere (Wang et al., 2014). Briefly, black lamps
118 (1.2m-long, 60W Philips/10R BL, Royal Dutch Philips Electronics Ltd, The
119 Netherlands) are used as light source, providing a NO_2 photolysis rate of 0.49 min^{-1}.
120 Two Teflon-coated fans are installed inside the reactor to guarantee well mixing of the
121 introduced gas species and particles within 120 seconds. Temperature can be set in the
122 range from −10 to 40 °C at accuracy of ±1 °C as measured by eight temperature
123 sensors inside the enclosure and one just inside the reactor. Relative humidity (RH)
124 inside the reactor is achieved by vaporizing Milli-Q ultrapure water contained in a 0.5
125 L Florence flask and then flushing the water vapor into the reactor with purified dry
126 air until target RH is reached. In the present study, temperature and RH inside the
127 reactor were all set to 25 ℃ and 50%, respectively. During the experiments, the top
128 frame is automatically lowered to maintain a differential positive pressure inside the
129 reactor against the enclosure to avoid the contamination of the enclosure air.

130 Gasoline vehicle exhausts were injected to the reactor through Teflon lines using
131 two oil-free pumps (Gast Manufacturing, Inc, USA) at a flow rate of 40 L min^{-1}. The
132 injection time varied from a few minutes to more than one hour based on the primary
133 emissions of different vehicles. A schematic of the smog chamber and the vehicle
134 exhaust injection system is shown in Fig. 1.

135 **2.2 Characterization of gas- and particle-phase chemical compositions and**
136 **particle sizes**

Gas-phase ozone (O_3) and NO_x were measured online with dedicated monitors (EC9810 and 9841T, Ecotech, Australia). Online monitoring of parent ~~NMHCs~~ VOCs such as C_6–C_{10} single-ring aromatic hydrocarbons and their oxidation products were available with a commercial proton-transfer-reaction time-of-flight mass spectrometer (PTR-TOF-MS, Model 2000, Ionicon Analytik GmbH, Austria). Detailed descriptions of the PTR-TOF-MS technique can be found elsewhere (Lindinger et al., 1998; Jordan et al., 2009). In this study the decay curve of toluene measured by PTR-TOF-MS were also used to derive the average hydroxyl radical (OH) concentration during each experiment. A wide spectrum of VOCs were also measured offline by drawing 250 ml air inside the reactor to a Model 7100 Preconcentrator (Entech Instruments Inc., USA) coupled with an Agilent 5973N gas chromatography-mass selective detector/flame ionization detector~~/electron capture detector~~ (GC-MSD/FID~~/ECD~~, Agilent Technologies, USA). Detailed descriptions of the method can be found elsewhere (Wang and Wu, 2008; Y. L. Zhang et al., 2010, 2012, 2013). C2-C3 and C4-C12 hydrocarbons were measured by GC-FID and GC-MSD, respectively. In this study, the offline measurement was the standard method to determine the mass concentrations of VOCs. PTR-TOF-MS was used for deriving the time-resolved concentrations of VOCs. The VOC concentrations measured offline were also used as an independent check of that measured online by the PTR-TOF-MS. To determine CO/ CO_2 concentrations before and after the introduction of exhausts, air samples were also collected into 2 L cleaned Teflon bags. CO was analyzed using a gas

chromatography (Agilent 6980GC, USA) with a flame ionization detector and a packed column (5A Molecular Sieve 60/80 mesh, 3 m × 1/8 inch) (Y. L. Zhang et al., 2012), and CO_2 was analyzed with a HP 4890D gas chromatography (Yi et al., 2007). The detection limits of CO and CO_2 were <30 ppb. The relative SDs were all less than 3% based on 7 duplicates running 1.0 ppm CO and CO_2 standards (Spectra Gases Inc, USA).

A high-resolution time-of-flight aerosol mass spectrometer (HR-TOF-MS, Aerodyne Research Incorporated, USA) was used to measure the particle chemical compositions (Jayne et al., 2000; DeCarlo et al., 2006). The instrument was operated in the high sensitivity V-mode and high resolution W-mode alternatively every two minutes. The toolkit Squirrel 1.51H was used to obtain time series of various mass components (sulfate, nitrate, ammonium and organics). We used the toolkit Pika 1.1H to determine the average element ratios of organics, like H:C, O:C, and N:C (Aiken et al., 2007, 2008). The contribution of gas-phase CO_2 to the m/z 44 signal was corrected using the measured CO_2 concentrations. The HR-TOF-MS was calibrated using 300 nm monodisperse ammonium nitrate particles.

Particle number/volume concentrations and size distributions were measured with a scanning mobility particle sizer (SMPS, TSI Incorporated, USA., classifier model 3080, CPC model 3775). Flow rates of sheath and aerosol flow were 3.0 and 0.3 L min^{-1}, respectively, allowing a size distribution scanning ranging from 14 nm to 700 nm within 255 s. The accuracy of the particle number concentration is ±10%. An

aerosol density of 1.4 g cm^{-3} was assumed to convert the particle volume concentration into the mass concentration (Zhang et al., 2005). Conductive silicon tubes were used as sampling lines for HR-TOF-MS and SMPS to reduce electrostatic losses of particles.

2.3 **Experimental procedure**

Two light-duty gasoline-powered vehicles were used in this study, one Euro 1 and one Euro 4 vehicles. They are both port fuel injected vehicles. More details of the vehicles are listed in Table 1. Both of the vehicles were fueled with Grade 93# gasoline, which complies with the Euro III gasoline fuel standard. Details of the oil compositions can be found in our previous study (Zhang et al., 2013).

Prior to each experiment, the reactor was evacuated and filled with purified dry air for at least 5 times, then the reactor was flushed with purified dry air for at least 48 h until no residual hydrocarbons, O_3, NO_x, or particles were detected in the reactor to avoid carry-over problems from day-to-day experiments. Prior to the introduction of exhaust, the temperature control system and Teflon coated fans were turned on. The exhaust could be injected when the temperature in the reactor was stable at the set temperature 25 ℃.

The LDGV was parked outside the laboratory and tested at idling. Before the injection of exhaust, the cars were at idling for at least half an hour to warm up the three-way catalysts, and then the vehicle exhausts were injected into the reactor. During the introduction, the raw exhausts were also sampled into 8 L cleaned

aluminum foil bags by a mechanical pump with a flow rate of about 5 L min^{-1}. VOCs and CO_2 –in these samples were measured offline by the same methods mentioned above to characterize the primary emissions from the exhaust pipe. The exhaust in the reactor was diluted by a factor of 13–30 compared to the tailpipe.

Additional NO was then added to adjust the VOC/NO_x ratios to around 10.0 or 2.0 (Table 2), within the range of 0.5–10 reported in gasoline vehicle exhaust tests and downwind urban areas (Clairotte et al., 2013). The initial concentrations of NO_x at the start of the experiments ranged from 134 to 956 ppb. In each experiment CH_3CN was used as an indicator of dilution in the reactor. After being characterized in the dark for more than 30 min, the exhaust was exposed to black light continuously for 5 h. After the black lamps were switched off, the formed SOA was characterized for another 2 to 3 h to correct the particles wall loss. Blank experiments with no vehicle exhaust introduced were performed to quantify the reactivity of the matrix gas. After 5 h of irradiation, the number and mass of formed particles were <5 cm^{-3} and 0.1 μg m^{-3}, respectively.

During the introduction of exhausts, particles and VOCs might deposit to the surface of the transfer lines. Therefore, a flow rate of as high as 20 L min^{-1} and a transfer line of as short as 5 m were used to provide residence time within seconds, and thus reduce the losses of particles and VOCs in the transfer lines. Furthermore, before being introduced into the reactor, exhausts were generally pumped through the transfer lines for half an hour to saturate the transfer lines with particles and VOCs

while warming the catalytic converter. Losses of particles and VOCs in the introduction lines were determined by comparing the concentrations of total particle number and VOCs in the directly emitted exhausts with the ones after passing through the transfer lines. The loss of total particle number was estimated to be less than 3%. The penetration efficiency of particles due to diffusion in a cylindrical tube, η(dp), can be also estimated by a laminar diffusional deposition model (Gormley and Kennedy, 1949). For particles with diameters larger than 10 nm, the penetration efficiency was higher than 95%, indicating minor losses of particles in the transfer line. The losses of VOCs in the transfer line were estimated to be less than 5%, which might lead to a small underestimation of SOA production.

2.4 Data analysis

2.4.1 Wall loss corrections

The loss of particles and organic vapors to the reactor walls has to be accounted for to accurately quantify the SOA formation. The loss of particles onto the walls has been well constrained and is treated as a first-order process (McMurry and Grosjean, 1985). The wall-loss rate constant was determined separately for each experiment by fitting the SMPS and AMS data with first-order kinetics when ~~no new particles were formed~~UV lamps were turned off. By applying this rate to the entire experiment, we use the same method as Pathak et al. (2007) treating the particle wall loss as a first order process to correct the wall loss of the particles. The wall loss of particles is a size-dependent process, therefore, the influence of nucleation need to be examined

due to the rapid loss of nucleation mode particles. In this study, the impact of the nucleation event on wall-loss estimate is considered to be negligible for only less than 3% of the particle mass is in the nucleation mode ten minutes after nucleation for all the experiments (Fig. ~~2~~S1 in the Supplement). In general, the loss of condensable organic vapors to the walls is estimated for two limiting cases (Weitkamp et al., 2007; Hildebrandt et al., 2009). In the first case (designated ω =0), no organic vapors is lost to the walls (only to suspended particles). In the second case (designated ω =1), the particles on the walls are in equilibrium with the organic vapors; therefore condensation to the particles on the walls is identical to the suspended particles. We use the ω =0 wall-loss correction assuming the organic vapors only condensation onto suspended particles. The ω =1 wall-loss correction is not suitable for the experiments here in which nucleation occurred and no seed particles were added (Henry et al., 2012).

2.4.2 AMS data corrections

Theoretically, the sum of the PM mass measured by AMS should be equal to the mass calculated from the SMPS mass size distributions. However, both ~~the two~~ methods have limitations. One must assume a particle shape and density to convert the volume concentration measured by SMPS to the mass concentration. Here, we assume that particles are spherical with an average density of 1.4 g cm^{-3} (Zhang et al., 2005). Fractal-like particles will cause the overestimate of the spherical equivalent diameter, thus overestimating the particle mass. AMS tends to underestimate the PM

mass due to the transmission efficiency (Liu et al., 2007) and the AMS collection efficiency (Gordon et al., 2014), leading to the discrepancy between the AMS data and SMPS data. Fig. S2 shows the particle volume distribution measured by SMPS for a typical smog chamber experiment (experiment 2). Most particles were in the range 40-120 nm after SOA formation. Since the transmission window of the standard lens of HR-TOF-AMS is 60-600 nm (aerodynamic diameter) (Liu et al., 2007), particles with diameter lower than 40 nm (mobility diameter) were cut from the lower edge of the volume distribution. After 1 h since nucleation occurred, only <5% of the mass was outside the transmission window of HR-TOF-MS, indicating that HR-TOF-AMS might underestimate the PM in the early stage of SOA formation. In this study, we use the same method as Gordon et al. (2014) to correct the AMS data.

For all the experiments with discrepancies between the AMS and SMPS data (Fig. S3), we assume that the difference in mass has the same composition as the measured components. We then calculate scaling factors, AMS_{sf}, to correct the PM mass measured by AMS and make it accordant with the SMPS measurements. The scaling factor is

$$AMS_{sf} = \frac{C_{SMPS}}{C_{Org} + C_{SO_4} + C_{NO_3} + C_{NH_4}} \quad (1)$$

where C_{SMPS} is the total particle mass concentration derived by the SMPS, C_{Org}, C_{SO4}, C_{NO3} and C_{NH4} are the mass concentrations of organics, sulfate, nitrate and ammonium measured by the AMS. As shown in Fig. S3, the mass of primary particles measured by SMPS was comparable with that measured by HR-TOF-AMS, thus we assumed

that the mass of black carbon (BC) in the reactor was negligible. The AMS_{sf} for each time step after nucleation is calculated and used to scale the AMS data for the entire experiment.

2.4.3 Effective SOA yields

To compare the SOA formation with other studies, we calculated effective SOA yields for all experiments. The effective SOA yield Y was defined as the ratio of the wall-loss-corrected SOA mass to the mass of reacted organic precursors (Odum et al., 1996, 1997; Donahue et al., 2006). In this study, reacted organic precursors included in calculation are only those quantified by GC-MSD, including benzene, toluene, C2–benzene, C3–benzene, C4-benzene and naphthalene. A detailed list of these compounds is presented in Table ~~3~~S2. At the beginning and end of each experiment, ~~simulating air~~air samples in the reactor were collected into 2 L electropolished and evacuated ~~2 L~~ stainless steel canisters and analyzed by GC-MSD to determine the mass of reacted organic precursors.

2.4.4 Emission factors

Emission factor (EF) of a pollutant P is calculated on a fuel basis (g kg^{-1}):

$$EF = 10^3 \bullet [\Delta P] \bullet \left(\frac{MW_{CO_2}}{[\Delta CO_2]} + \frac{MW_{CO}}{[\Delta CO]} + \frac{MW_{HC}}{[\Delta HC]}\right) \bullet \frac{\omega_C}{MW_C} \quad (2)$$

where $[\Delta P]$, $[\Delta CO_2]$, $[\Delta CO]$, and $[\Delta HC]$ are the background corrected concentrations of P, CO_2, CO and the total hydrocarbons in the reactor in μg m^{-3}; MW_{CO2}, MW_{CO}, MW_{HC}, and MW_C are the molecular weights of CO_2, CO, HC and C. ω_C (0.85) is the carbon intensity of the gasoline (Kirchstetter et al., 1999).

2.4.5 Determination of OH exposure

Decay of toluene measured by PTR-TOF-MS is used to derive the average OH concentration during each experiment. Changes in the toluene concentration over time can be expressed as:

$$\frac{d[toluene]}{dt} = -k \cdot [OH] \cdot [toluene] \quad (3)$$

where k is the ~~reaction~~ rate constant for the reaction between toluene and OH radical. Assuming a constant OH concentration during an experiment, we can integrate Eq. (3) to get Eq. (4):

$$\ln\left(\frac{[toluene]_0}{[toluene]_t}\right) = k \cdot [OH] \cdot t \quad (4)$$

So ~~B~~by plotting $ln([toluene]_0/[toluene]_t)$~~the natural logarithm (ln) of the ratio between the initial toluene concentration and the toluene concentration at time t~~ versus time t, we can obtain a slope that equals $k \times [OH]$~~$k \cdot [OH]$~~. The average OH concentration is therefore calculated as:

$$[OH] = \frac{slope}{k} \quad (5)$$

The OH exposure is then determined through multiplying the average OH concentration by time.

3. Results and discussion

3.1 VOC composition

Fig. ~~4~~ 2 shows the average composition of gasoline vehicle exhausts from vehicle I

(Euro 4) and II (Euro 1). For Euro 4 and 1 vehicle ~~I and II~~, alkanes ~~shared~~ contributed about 42.9% and 66.2% of the total speciated ~~NMHCs~~ VOCs measured with the GC-FID/MSD by mass, respectively, dominating the ~~NMHCs~~ speciated VOCs emissions in gasoline vehicle exhausts. Due to the high concentrations of isopentane and methylpentane, branched alkanes contributed approximately 44.9% of the total ~~NMHCs~~ VOCs for Euro 1 vehicle ~~II~~, quite higher than that for Euro 4 vehicle ~~I~~ (23.3%). Aromatic hydrocarbons accounted for about 38.0% and 22.5% of the total ~~NMHCs~~ VOCs for Euro 4 and 1 vehicle ~~I and II~~, respectively, relatively higher than 10-15% observed by Nordin et al. (2013) for idling Euro 2, 3 and 4 vehicles. The mass fraction of aromatic hydrocarbons for Euro 4 vehicle was comparable with 32.2% for idling private cars in Hong Kong (Guo et al., 2011) and 38.3% for Euro 3 light-duty gasoline vehicles operated through ECE cycles with an average speed around 18.7 km h^{-1} (Wang et al., 2013). Both Schauer et al. (2002) and Gentner et al. (2013) observed that aromatic hydrocarbons contributed around 27% of the total VOCs for gasoline-powered automobiles driven through the cold-start Federal Test Procedure urban driving cycle and on-road gasoline vehicles in the Caldecott tunnel, similar with that of Euro 1 vehicle. Recently, Huang et al. (2015) reported that mass fractions of aromatic hydrocarbons were as high as 46.4% for Euro 1, 2, and 3 light-duty gasoline vehicles operated through ECE cycles. Therefore, t~~T~~he variations of the composition of LDGV exhausts in this study were within the range of previous studies. ~~may be due to the difference of the fuel, vehicle type and emission standard.~~

The averaged emission factors of ~~NMHCs~~ VOCs and aromatic hydrocarbons for Euro 4 vehicle ~~I~~ were 2.1 and 0.8 g kg^{-1}, approximately 26.0% and 43.5% of ~~1.3 and 0.5 times lower than~~ those for Euro 1 vehicle ~~II~~, respectively. Compared with a Euro 5 gasoline vehicle operated during a New European Driving Cycle, the emission factor of ~~NMHCs~~ VOCs for ~~vehicle I~~Euro 4 vehicle was about 1.7 times higher (Platt et al., 2013). Using 7.87 L/100 km as the average fuel efficiency (Wagner et al., 2009), we obtained the VOCs emission factors based on g km^{-1} for Euro 4 and 1 vehicles to be 0.12 and 0.46 g km^{-1}, respectively, comparable with the previous reported values for Euro 1 and 4 gasoline vehicles in China (Huo et al., 2012; Huang et al., 2015). According to previous studies, ~~T~~there is a clear reduction of ~~primary~~ VOCs emissions from gasoline vehicles with stricter emission standards (Huo et al., 2012; Huang et al., 2015). It is worth noting that emissions of HC from gasoline vehicles during idling were observed to be lower than those in the acceleration and deceleration modes (Tong et al., 2000; Yamamoto et al., 2012; Huang et al., 2013), but in a similar level with those in the cruising mode (Tong et al., 2000). It is important to note that the reported data are only based on five chamber experiments with two LDGVs under idling conditions. More tests are needed to assess SOA formation from gasoline vehicle exhausts in China.

3.2 SOA formation

Fig. ~~5~~ 3 shows the temporal evolution of gas–phase and particle–phase species during a typical smog chamber experiment. During -1.3 h to -0.85 h, the vehicle exhausts

were introduced into the reactor. At time = -0.55 h, the relative humidity was adjusted to approximately 40%, and HR-TOF-AMS was connected to characterize the primary PM. NO was injected to adjust the VOC/NO_x ratio at approximately time = -0.25 h. After the black lamps were turned on, NO was fast converted to NO_2 in less than 1 h, and then O_3 was accumulated and OH radical was formed. When NO concentration decreased to a low level about 5 ppb, gas-phase light aromatics especially C_3–benzene with higher reactivity, decayed rapidly due to the reaction with OH radical. SOA was thus rapidly formed and increased to a high level in less than 2 h. As shown in Table 43, at the end of all the experiments, the formed SOA was 12–259 times as high as POA. This enhancement is consistent with 9–500 recently reported by Nordin et al. (2013) when studying SOA formation from idling European gasoline passenger vehicle emissions. As shown in Fig. 5c3c, the total particle number concentration increased fast from 82 to 116143 cm^{-3} ~~in approximately 10 min~~, indicating dramatic new particle formation~~.~~, which might be due to that the starting surface concentrations of particles were all below a critical value (100–2000 μm^2 cm^{-3}, Table S1) (Wehner et al., 2004). As shown in Table S1, primary particle numbers in the reactor in this study ranged from 82 to 18948 cm^{-3}, 1-2 orders of magnitude higher than that of a Euro 2 car operated at idling with a similar dilution ratio (Nordin et al., 2013), indicating that the small starting particle number concentrations might mainly due to the idling condition of tested cars rather than the losses in the introduction lines. In addition, upon entering into the chamber, emitted particles would partition due to dilution

similar as in the atmosphere, regardless of the temperature and concentration in the sampling system, which might lead to the decrease of starting number concentrations. A certain extent of primary particles under the detection limit of 14 nm of SMPS also contributed to the measured small starting number concentration of particles. ~~After nucleation occured, the mean diameter increased from 20 to 60 nm in about 1.5 h. Because particles with diameters lager than 50 nm can act as cloud condensation nuclei (CCN) (McFiggans et al., 2006) and influence the radiative forcing, SOA from vehicle exhausts may has climate effects to a certain extent as well as air quality effects.~~

Deposition of SOA-forming vapors to the walls might lead to the underestimation of SOA production. The wall loss rate coefficient of vapors is related with the numbers of carbon and oxygen in the molecule (X. Zhang et al., 2015). Here, we take $C_7H_8O_4$, a product of the photo-oxidation of toluene as an example. The loss of $C_7H_8O_4$ to walls would be 7% in an hour before SOA formation when a wall deposition rate of 2×10^{-5} s^{-1} was used (X. Zhang et al., 2015). After SOA formation, the surface concentrations of particles increased fast to as high as 2000 μm^2 cm^{-3} in an hour, which would reduce the vapor wall losses.

SOA production factors (PF) for the LDGVs ~~in China~~tested in this study were estimated to vary from 0.001 to 0.044g kg^{-1} fuel, which are within the results of Nordin et al. (2013) and Gordon et al. (2014) with OH exposure around 5.0×10^6 molecules cm^{-3} h. A recent study investigating SOA formation from in-use vehicle

emissions in a highway tunnel in Pittsburg indicated that the peak SOA production was measured at an OH exposure of 1.9×10^{8} molecules cm^{-3} h and current smog chamber studies may underestimate the ultimate SOA production by a maximum factor of about 10 due to the limited OH exposure (Tkacik et al., 2014).

~~Decay of toluene measured by PTR-TOF-MS is used to derive the average OH concentration during each experiment. Changes in the toluene concentration over time can be expressed as:~~

$$\frac{d[toluene]}{dt} = -k\cdot[OH]\cdot[toluene] \quad (3)$$

~~where k is the reaction rate constant between toluene and OH radical. Assuming a constant OH concentration during an experiment, we can integrate Eq. (3) to get Eq. (4):~~

$$\ln(\frac{[toluene]_0}{[toluene]_t}) = k\cdot[OH]\cdot t \quad (4)$$

~~By plotting the natural logarithm (ln) of the ratio between the initial toluene concentration and the toluene concentration at time t versus time, we can obtain a slope that equals $k\cdot[OH]$. The average OH concentration is therefore:~~

$$[OH] = \frac{slope}{k} \quad (5)$$

The average OH radical concentration (Table ~~4~~3) was determined to be 0.79-1.23$\times$ 10^{6} molecules cm^{-3} during our experiments. This OH level was about ten times lower than the average OH concentration of 1.5×10^{7} molecules cm^{-3} around noon in summer in the Pearl River Delta, China (Hofzumahaus et al., 2009). The OH exposure in this study is only 5×10^{6} molecules cm^{-3} h, equivalent to 0.3 hour of atmospheric

oxidation. Therefore, the real-world SOA production factor from LDGVs in the atmosphere in China may be even higher than our estimation.

3.3 SOA yield

Effective SOA yield from vehicle exhaust calculated as described in 2.4.3 ranged from 2.8% to 17.2%. Pankow (1994 a, b) and Odum et al. (1996) indicated that Y is a function of M_0 and the relation is described as:

$$Y = M_0 \sum \left(\frac{\alpha_i K_{om,i}}{1 + K_{om,i} M_0}\right) \quad (6)$$

where $K_{om,i}$ and α_i are the mass-based absorption equilibrium partitioning coefficient and stoichiometric coefficient of product i, respectively; M_0 is the total mass concentration of organic material. As shown in Table 3, SOA yields for Euro 1 vehicle were around 3%, quite lower than 10%-17% for Euro 4 vehicle. The mass fraction of aromatic hydrocarbons for Euro 4 vehicle was about two times higher than that for Euro 1 vehicle (Fig. 2a), which would form more semi-volatile organic compounds (SVOCs) partitioning into particle phase under similar OH exposure and thus lead to the relatively higher SOA yields.

Comparison of effective yield data obtained for the LDGV exhaust in this study with those of Nordin et al. (2013) is shown in Fig. ~~6~~4. Effective yield data of this study are well fit with the one-product model, namely $Y = M_0 \left(\frac{\alpha_1 K_{om,1}}{1 + K_{om,1} M_0}\right)$. The appropriate values for α_1 and $K_{om,1}$ when fitting the yields are 0.350 ± 0.114 and 0.007 ± 0.004, respectively. The effective SOA yields in the study of Nordin et al. (2013)

were 60%-360% higher than those in this study at same concentrations of M_0. In their calculation of the reacted SOA precursors, C4-benzene and naphthalene were excluded. The effective SOA yields would increase 7%-34% when C4-benzene and naphthalene were excluded in this study, which could explain a small portion of the discrepancy. According to the estimation above, the loss of VOCs in the transfer lines was less than 5%. A little higher than VOCs, if assumed to be 20%, losses of IVOCs and SVOCs in the transfer lines would increase the SOA effective yields by a factor of 2%-10% when the unexplained SOA discussed later was all attributed to the contribution from IVOCs and SVOCs. The existence of seed particles in the study of Nordin et al. (2013) might reduce the wall loss of semi-volatile organic vapors and thus increase the effective SOA yield (Kroll et al., 2007; Zhang et al., 2014; X. Zhang et al., 2015). However, Cocker et al. (2001) found that SOA formation from m-xylene and 1,3,5-trimethylbenzene photo-oxidation was unaffected by the presence of ammonium sulfate seed aerosols. The influence of seed particles on SOA yields still needs further investigations. Faster oxidation rates caused by higher OH concentrations in the study of Nordin et al. (2013) would also result in higher SOA yields (Ng et al., 2007).~~Compared with the study of Nordin et al. (2013), the effective SOA yield in this study were relatively lower when the M_0 is equal. Ammonium sulfate was added as the seed aerosol by Nordin et al. (2013). Previous studies showed that SOA yields from the photooxidation of aromatics hydrocarbons were lower without the presence of inorganic seed particles (Kroll et al., 2007; Lu et al., 2009).~~

~~The average OH concentration is relatively lower than that in the study of Nordin et al. (2013). Ng et al. (2007) indicated that faster oxidation rates caused by higher OH concentrations would result in higher SOA yields.~~ Additionally, the different VOCs profiles of exhausts might also influence the SOA yields.

SOA production from the reacted organic precursors can be estimated by the following formula:

$$\Delta \mathrm{SOA}_{predicted} = \sum_{j} (\Delta X_j \times Y_j) \quad (7)$$

where $\Delta \mathrm{SOA}_{predicted}$ is the predicted SOA concentration in μg m^{-3}; ΔX_j is the mass of reacted aromatic hydrocarbon X_j in μg m^{-3}; and Y_j is the corresponding SOA yield of X_j. In this study, the SOA yield of benzene and other single-ring aromatics were estimated using the two-product model curves taken from Borrás et al. (2012) and Odum et al. (1997), respectively. While the SOA yield of naphthalene was taken from Shakya et al. (2010). SOA yield curves of toluene and m-xylene from Ng et al. (2007) were also widely used to estimate SOA production (Platt et al., 2013). However, the introduction of seed aerosols and OH precursor made the SOA yield curves in the study of Ng et al. (2007) not suitable for this study. Considering that the study of Odum et al. (1997) provided a systematic estimation of SOA yields from toluene, C2-benzene, C3-benzene and C4-benzene, we mainly used the two-product curves from Odum et al. (1997) to estimate the SOA production. The aerosol yield curves from literature were converted to the same aerosol density of 1.4 g cm^{-3} as this study. The SOA yield for each precursor was calculated for the measured concentration of

OA in the reactor. Then the predicted SOA production from each precursor can be calculated (Table ~~3~~S2).

Fig. ~~7~~ 5 shows the contributions of the predicted benzene SOA, toluene SOA, C_2–benzene SOA, C_3–benzene SOA, C_4–benzene SOA and naphthalene SOA to the total measured SOA in all experiments. C_4–benzene contributed negligible SOA because of the very low emissions of C_4–benzene from light-duty gasoline vehicles (~~Table 5~~Fig. 2b). Though benzene took relatively higher percentage of the total ~~NMHCs~~VOCs, benzene also accounted for a negligible proportion of the formed SOA due to its low reactivity with OH radicals. Naphthalene was previously estimated to contribute around 5% of the vehicle SOA mass (Nordin et al., 2013). While in this study naphthalene was calculated to contribute 8%–52% of the formed SOA. The initial concentrations of naphthalene in this study ranged from 8.5 to 39.5 ppb, much higher than 2.8–4.4 ppb in the study of Nordin et al. (2013). The high contributions of naphthalene are probably attributed to its relatively higher initial concentrations and higher mass yield than single-ring aromatics for similar experimental conditions (Odum et al., 1997; Ng et al., 2007).

Totally, single-ring aromatics and naphthalene accounted for 51%–90% of the measured SOA, comparable to the estimation that classical C6–C9 light aromatics were responsible for 60% of the formed SOA from gasoline vehicle exhausts (Nordin et al., 2013), indicating that there are other SOA precursors in the LDGV exhausts. Platt et al. (2013) attributed the unexplained SOA formed from the aging of emissions

from a Euro 5 gasoline car to highly oxygenated hydrocarbons. In addition, ~~intermediate-volatility organic compounds (~~IVOCs~~)~~ such as branched and cyclic alkanes were recognized as important SOA precursors derived from wood burning, diesel engine and aircraft exhaust (Robinson et al., 2007; Weitkamp et al., 2007; Grieshop et al., 2009; Tkacik et al., 2012). Gordon et al. (2014) found that unspeciated species including branched and cyclic alkanes contributed about 30% of the nonmethane organic gas emissions from LDGVs with model years of 1995 or later and be associated with the majority of the SOA formation. Tkacik et al. (2014) also found that unspeciated species were predicted to contribute twice as much SOA from in-use vehicle emissions as traditional precursors. It is worth noting that photooxidation of aromatic hydrocarbons in a complex mixture such as gasoline vehicle exhausts might alter the SOA yield compared to pure precursor experiments, thus probably influencing the estimation in this study (Song et al., 2007). Wall losses of organic vapors were not considered in this study, which would lead to the underestimation of SOA production. Therefore, the mass closure analysis estimated the maximum amount of SOA that could be explained by aromatics.

3.4 SOA composition

Fragmentations derived from the AMS data have been widely used to explore the oxidation degree of the organic aerosols (Zhang et al., 2005; Ng et al., 2010; Heald et al., 2010). The usually used ion fragments include m/z 43, 44 and 57. The dominating organic peaks in gasoline vehicle exhaust SOA are m/z 43 and 44 (Nordin et al.,

2013), while m/z 57 is a main hydrocarbon fragment in diesel SOA (Chirico et al., 2010). Here, we use the approach of Ng et al. (2010) by plotting the fractions of total organic signal at m/z 43 (f_{43}) vs. m/z 44 (f_{44}) together with the triangle defined according to the analysis of ambient AMS data. The m/z 43 signal includes $C_3H_7^+$ and $C_2H_3O^+$ ions, indicating fresh less oxidized organic aerosols. The m/z 44 signal, dominated by CO_2^+ and formed from the thermal decarboxylation of organic acids, is an indicator of highly oxygenated organic aerosols (Ng et al., 2010).

Fig. ~~8a~~ 6a shows the f_{43} vs. f_{44} at the end of each experiment and the results of Nordin et al. (2013) and Presto et al. (2014), together with the triangle developed by Ng et al. (2010). The ambient low-volatility oxygenated OA (LV-OOA) and semi-volatile OOA (SV-OOA) factors fall in the upper and lower portions of the triangle, respectively. Our data mainly lie in the SV-OOA region, similar to the results of Nordin et al. (2013) and Presto et al. (2014). However, SOA in one experiment show relatively lower oxidation degree. This phenomenon reflects the different SOA compositions among different experiments and might be caused by the different VOCs profiles, OH exposure and organic mass loadings (Ng et al., 2010).

The O:C ratio can also be used to characterize the oxidation degree of the organic aerosols. After 5 h irradiation the H:C ratios varied from 1.22 to 1.37 and the O:C ratios from 0.43 to 0.69 for all the experiments. Almost all the O:C values were lower than 0.6, comparable to the SV-OOA compounds, which typically has O:C ratios between 0.3 and 0.6 (Jimenez et al., 2009). Platt et al. (2013) observed a

555 relatively higher O:C ratio of 0.7 on the aging (OH = 12×10^6 molecules cm^{-3} h) of
556 emissions from a Euro 5 gasoline car operated during a New European Driving Cycle.
557 As a higher OH exposure will lead to a higher O:C ratio, if the gasoline exhaust in this
558 study was irradiated under a similar OH exposure to that of Platt et al. (2013) , the
559 O:C ratios might reach to the similar level or higher, comparable to the LV-OOA
560 factor (Jimenez et al., 2009).

561 In Fig. ~~8b~~ 6b we plot the O:C and H:C molar ratios after SOA was formed during
562 experiments 1, 2 and 3 on a Van Krevelen diagram (Heald et al., 2010). The slopes
563 ranged from -0.59 to -0.36, similar to previous laboratory studies of Tkacik et al.
564 (2012) for cyclic, linear and branched alkanes, Jathar et al. (2013) for unburned fuel
565 and Presto et al. (2014) for light-duty gasoline vehicle exhaust. They are also similar
566 to the ambient data (Ng et al., 2011). A slope of -1, -0.5 and 0 in the Van krevelen
567 diagram represents the addition of alcohol/peroxide, the addition of carboxylic acid
568 with fragmentation, and the addition of carboxylic acid without fragmentation,
569 respectively (Heald et al., 2010; Ng et al., 2011). Consequently, the slopes in this
570 study indicate that the SOA formation is a combination of the addition of both
571 carboxylic acid and alcohol/peroxide function groups without C-C bond cleavage
572 and/or the addition of carboxylic acid with C-C bond breakage (Heald et al., 2010; Ng
573 et al., 2011).

574 ~~**4. Conclusion**~~

575 ~~Better understanding of the magnitude and property of SOA formed from exhausts of~~

~~vehicles in China will provide valuable information to the government and climate modelers. As presented in this study, gasoline vehicle exhaust SOA was fast formed and extremely exceeded the POA. Traditional single-ring aromatic precursors and naphthalene could explain 51%–90% of the formed SOA. Unspeciated species such as branched and cyclic alkanes might be the possible precursors for the unexplained SOA. More work is needed to better understand the role of LDGVs on the fossil SOA in the atmosphere by studying the SOA formation of emissions from more vehicles with different model years, types and emission standards. Furthermore, given that the emissions from gasoline vehicles vary a lot with the driving conditions, the SOA formation of emissions from LDGVs in China under 'real world' conditions is needed to be investigated in the future.~~

Acknowledgments

This study was supported by National Natural Science Foundation of China (Project No. 41025012/41121063), Strategic Priority Research Program of the Chinese Academy of Sciences (Grant No. XDB05010200), NSFC-Guangdong Joint Funds (U0833003) and Guangzhou Institute of Geochemistry (GIGCAS 135 project Y234161001).

References

Aiken, A. C., DeCarlo, P. F., and Jimenez, J. L.: Elemental Analysis of Organic Species with Electron Ionization High-Resolution Mass Spectrometry, Anal. Chem., 79, 8350-8358, 10.1021/ac071150w, 2007.

Aiken, A. C., DeCarlo, P. F., Kroll, J. H., Worsnop, D. R., Huffman, J. A., Docherty, K. S., Ulbrich, I. M., Mohr, C., Kimmel, J. R., Sueper, D., Sun, Y., Zhang, Q., Trimborn, A., Northway, M., Ziemann, P. J., Canagaratna, M. R., Onasch, T. B., Alfarra, M. R., Prevot, A. S. H., Dommen, J., Duplissy, J., Metzger, A., Baltensperger, U., and Jimenez, J. L.: O/C and OM/OC ratios of primary, secondary, and ambient organic aerosols with high-resolution time-of-flight aerosol mass spectrometry, Environ. Sci. Technol., 42, 4478-4485, 10.1021/es703009q, 2008.

Borrás, E., and Tortajada-Genaro, L. A.: Secondary organic aerosol formation from the photo-oxidation of benzene, Atmos. Environ., 47, 154-163, 2012.

Cao, J. J., Lee, S. C., Ho, K. F., Zhang, X. Y., Zou, S. C., Fung, K., Chow, J. C., and Watson, J. G.: Characteristics of carbonaceous aerosol in Pearl River Delta Region, China during 2001 winter period, Atmos. Environ., 37, 1451-1460, Doi 10.1016/S1352-2310(02)01002-6, 2003.

Chan, C. K., and Yao, X.: Air pollution in mega cities in China, Atmos. Environ., 42, 1-42, http://dx.doi.org/10.1016/j.atmosenv.2007.09.003, 2008.

Chirico, R., DeCarlo, P. F., Heringa, M. F., Tritscher, T., Richter, R., Prévôt, A. S. H., Dommen, J., Weingartner, E., Wehrle, G., Gysel, M., Laborde, M., and Baltensperger, U.: Impact of aftertreatment devices on primary emissions and

secondary organic aerosol formation potential from in-use diesel vehicles: results from smog chamber experiments, Atmos. Chem. Phys., 10, 11545-11563, 10.5194/acp-10-11545-2010, 2010.

Clairotte, M., Adam, T. W., Zardini, A. A., Manfredi, U., Martini, G., Krasenbrink, A., Vicet, A., Tournie, E., and Astorga, C.: Effects of low temperature on the cold start gaseous emissions from light duty vehicles fuelled by ethanol-blended gasoline, Appl. Energ., 102, 44–54, 2013.

Cocker Iii, D. R., Mader, B. T., Kalberer, M., Flagan, R. C., and Seinfeld, J. H.: The effect of water on gas–particle partitioning of secondary organic aerosol: II. m-xylene and 1,3,5-trimethylbenzene photooxidation systems, Atmos Environ, 35, 6073-6085, http://dx.doi.org/10.1016/S1352-2310(01)00405-8, 2001.

de Gouw, J. A., Middlebrook, A. M., Warneke, C., Goldan, P. D., Kuster, W. C., Roberts, J. M., Fehsenfeld, F. C., Worsnop, D. R., Canagaratna, M. R., Pszenny, A. A. P., Keene, W. C., Marchewka, M., Bertman, S. B., and Bates, T. S.: Budget of organic carbon in a polluted atmosphere: Results from the New England Air Quality Study in 2002, J. Geophys. Res., 110, D16305, 10.1029/2004JD005623, 2005.

DeCarlo, P. F., Kimmel, J. R., Trimborn, A., Northway, M. J., Jayne, J. T., Aiken, A. C., Gonin, M., Fuhrer, K., Horvath, T., Docherty, K. S., Worsnop, D. R., and Jimenez, J. L.: Field-Deployable, High-Resolution, Time-of-Flight Aerosol Mass Spectrometer, Analytical Chemistry, 78, 8281-8289, 10.1021/ac061249n, 2006.

637 Donahue, N. M., Robinson, A. L., Stanier, C. O., and Pandis, S. N.: Coupled
638 partitioning, dilution, and chemical aging of semivolatile organics, Environ. Sci.
639 Technol., 40, 2635-2643, 10.1021/es052297c, 2006.
640 Donahue, N. M., Robinson, A. L., and Pandis, S. N.: Atmospheric organic particulate
641 matter: From smoke to secondary organic aerosol, Atmos. Environ., 43, 94-106,
642 http://dx.doi.org/10.1016/j.atmosenv.2008.09.055, 2009.
643 Duan, F. K., He, K. B., Ma, Y. L., Jia, Y. T., Yang, F. M., Lei, Y., Tanaka, S., and
644 Okuta, T.: Characteristics of carbonaceous aerosols in Beijing, China, Chemosphere,
645 60, 355-364, DOI 10.1016/j.chemosphere.2004.12.035, 2005.
646 Duan, F. K., Liu, X. D., He, K. B., Li, Y. W., and Dong, S. P.: Characteristics and
647 source identification of particulate matter in wintertime in Beijing, Water Air Soil
648 Poll, 180, 171-183, DOI 10.1007/s11270-006-9261-4, 2007.
649 Gentner, D. R., Worton, D. R., Isaacman, G., Davis, L. C., Dallmann, T. R., Wood, E.
650 C., Herndon, S. C., Goldstein, A. H., and Harley, R. A.: Chemical Composition of
651 Gas-Phase Organic Carbon Emissions from Motor Vehicles and Implications for
652 Ozone Production, Environ. Sci. Technol., 47, 11837-11848,
653 doi:10.1021/es401470e, 2013.
654 Gordon, T. D., Presto, A. A., May, A. A., Nguyen, N. T., Lipsky, E. M., Donahue, N.
655 M., Gutierrez, A., Zhang, M., Maddox, C., Rieger, P., Chattopadhyay, S.,
656 Maldonado, H., Maricq, M. M., and Robinson, A. L.: Secondary organic aerosol
657 formation exceeds primary particulate matter emissions for light-duty gasoline

vehicles, Atmos. Chem. Phys., 14, 4661-4678, 10.5194/acp-14-4661-2014, 2014.

Gormley, P. G., and Kennedy, M.: Diffusion from a Stream Flowing through a Cylindrical Tube, Proceedings of the Royal Irish Academy. Section A: Mathematical and Physical Sciences, 52, 163-169, doi:10.2307/20488498, 1949.

Guo, H., Zou, S. C., Tsai, W. Y., Chan, L. Y., and Blake, D. R.: Emission characteristics of nonmethane hydrocarbons from private cars and taxis at different driving speeds in Hong Kong, Atmos. Environ., 45, 2711-2721, http://dx.doi.org/10.1016/j.atmosenv.2011.02.053, 2011.

Hagler, G. S., Bergin, M. H., Salmon, L. G., Yu, J. Z., Wan, E. C. H., Zheng, M., Zeng, L. M., Kiang, C. S., Zhang, Y. H., Lau, A. K. H., and Schauer, J. J.: Source areas and chemical composition of fine particulate matter in the Pearl River Delta region of China, Atmos. Environ., 40, 3802-3815, DOI 10.1016/j.atmosenv.2006.02.032, 2006.

Hallquist, M., Wenger, J. C., Baltensperger, U., Rudich, Y., Simpson, D., Claeys, M., Dommen, J., Donahue, N. M., George, C., Goldstein, A. H., Hamilton, J. F., Herrmann, H., Hoffmann, T., Iinuma, Y., Jang, M., Jenkin, M. E., Jimenez, J. L., Kiendler-Scharr, A., Maenhaut, W., McFiggans, G., Mentel, T. F., Monod, A., Prévôt, A. S. H., Seinfeld, J. H., Surratt, J. D., Szmigielski, R., and Wildt, J.: The formation, properties and impact of secondary organic aerosol: current and emerging issues, Atmos. Chem. Phys., 9, 5155-5236, 10.5194/acp-9-5155-2009, 2009.

He, K., Yang, F., Ma, Y., Zhang, Q., Yao, X., Chan, C. K., Cadle, S., Chan, T., and Mulawa, P.: The characteristics of $PM_{2.5}$ in Beijing, China, Atmos. Environ., 35, 4959-4970, http://dx.doi.org/10.1016/S1352-2310(01)00301-6, 2001.

Heald, C. L., Jacob, D. J., Park, R. J., Russell, L. M., Huebert, B. J., Seinfeld, J. H., Liao, H., and Weber, R. J.: A large organic aerosol source in the free troposphere missing from current models, Geophys. Res. Lett., 32, L18809, 10.1029/2005GL023831, 2005.

Heald, C. L., Kroll, J. H., Jimenez, J. L., Docherty, K. S., DeCarlo, P. F., Aiken, A. C., Chen, Q., Martin, S. T., Farmer, D. K., and Artaxo, P.: A simplified description of the evolution of organic aerosol composition in the atmosphere, Geophys. Res. Lett., 37, L08803, 10.1029/2010gl042737, 2010.

Henry, K. M., Lohaus, T., and Donahue, N. M.: Organic Aerosol Yields from α-Pinene Oxidation: Bridging the Gap between First-Generation Yields and Aging Chemistry, Environ Sci Technol, 46, 12347-12354, 10.1021/es302060y, 2012.

Hildebrandt, L., Donahue, N. M., and Pandis, S. N.: High formation of secondary organic aerosol from the photo-oxidation of toluene, Atmos. Chem. Phys., 9, 2973-2986, 10.5194/acp-9-2973-2009, 2009.

Hofzumahaus, A., Rohrer, F., Lu, K., Bohn, B., Brauers, T., Chang, C.-C., Fuchs, H., Holland, F., Kita, K., Kondo, Y., Li, X., Lou, S., Shao, M., Zeng, L., Wahner, A., and Zhang, Y.: Amplified Trace Gas Removal in the Troposphere, Science, 324, 1702-1704, 10.1126/science.1164566, 2009.

Huang, C., Lou, D. M., Hu, Z. Y., Feng, Q., Chen, Y. R., Chen, C. H., Tan, P. Q., and Yao, D.: A PEMS study of the emissions of gaseous pollutants and ultrafine particles from gasoline- and diesel-fueled vehicles, Atmos Environ, 77, 703-710, DOI 10.1016/j.atmosenv.2013.05.059, 2013.

Huang, C., Wang, H. L., Li, L., Wang, Q., Lu, Q., de Gouw, J. A., Zhou, M., Jing, S. A., Lu, J., and Chen, C. H.: VOC species and emission inventory from vehicles and their SOA formation potentials estimation in Shanghai, China, Atmos. Chem. Phys. Discuss., 15, 7977-8015, 10.5194/acpd-15-7977-2015, 2015.

Huo, H., Yao, Z., Zhang, Y., Shen, X., Zhang, Q., Ding, Y., and He, K.: On-board measurements of emissions from light-duty gasoline vehicles in three mega-cities of China, Atmos. Environ., 49, 371-377, doi:10.1016/j.atmosenv.2011.11.005, 2012.

Jathar, S. H., Miracolo, M. A., Tkacik, D. S., Donahue, N. M., Adams, P. J., and Robinson, A. L.: Secondary Organic Aerosol Formation from Photo-Oxidation of Unburned Fuel: Experimental Results and Implications for Aerosol Formation from Combustion Emissions, Environ Sci Technol, 47, 12886-12893, 10.1021/es403445q, 2013.

Jathar, S. H., Gordon, T. D., Hennigan, C. J., Pye, H. O. T., Pouliot, G., Adams, P. J., Donahue, N. M., and Robinson, A. L.: Unspeciated organic emissions from combustion sources and their influence on the secondary organic aerosol budget in the United States, Proceedings of the National Academy of Sciences, 111,

721 10473-10478, 10.1073/pnas.1323740111, 2014.
722 Jayne, J. T., Leard, D. C., Zhang, X., Davidovits, P., Smith, K. A., Kolb, C. E., and
723 Worsnop, D. R.: Development of an Aerosol Mass Spectrometer for Size and
724 Composition Analysis of Submicron Particles, Aerosol. Sci. Tech., 33, 49-70,
725 10.1080/027868200410840, 2000.
726 Jimenez, J. L., Canagaratna, M. R., Donahue, N. M., Prevot, A. S. H., Zhang, Q.,
727 Kroll, J. H., DeCarlo, P. F., Allan, J. D., Coe, H., Ng, N. L., Aiken, A. C., Docherty,
728 K. S., Ulbrich, I. M., Grieshop, A. P., Robinson, A. L., Duplissy, J., Smith, J. D.,
729 Wilson, K. R., Lanz, V. A., Hueglin, C., Sun, Y. L., Tian, J., Laaksonen, A.,
730 Raatikainen, T., Rautiainen, J., Vaattovaara, P., Ehn, M., Kulmala, M., Tomlinson, J.
731 M., Collins, D. R., Cubison, M. J., E., Dunlea, J., Huffman, J. A., Onasch, T. B.,
732 Alfarra, M. R., Williams, P. I., Bower, K., Kondo, Y., Schneider, J., Drewnick, F.,
733 Borrmann, S., Weimer, S., Demerjian, K., Salcedo, D., Cottrell, L., Griffin, R.,
734 Takami, A., Miyoshi, T., Hatakeyama, S., Shimono, A., Sun, J. Y., Zhang, Y. M.,
735 Dzepina, K., Kimmel, J. R., Sueper, D., Jayne, J. T., Herndon, S. C., Trimborn, A.
736 M., Williams, L. R., Wood, E. C., Middlebrook, A. M., Kolb, C. E., Baltensperger,
737 U., and Worsnop, D. R.: Evolution of Organic Aerosols in the Atmosphere, Science,
738 326, 1525-1529, 10.1126/science.1180353, 2009.
739 Johnson, D., Utembe, S. R., Jenkin, M. E., Derwent, R. G., Hayman, G. D., Alfarra,
740 M. R., Coe, H., and McFiggans, G.: Simulating regional scale secondary organic
741 aerosol formation during the TORCH 2003 campaign in the southern UK, Atmos.

742 Chem. Phys., 6, 403-418, 10.5194/acp-6-403-2006, 2006.
743 Jordan, A., Haidacher, S., Hanel, G., Hartungen, E., Mark, L., Seehauser, H.,
744 Schottkowsky, R., Sulzer, P., and Mark, T. D.: A high resolution and high sensitivity
745 proton-transfer-reaction time-of-flight mass spectrometer (PTR-TOF-MS), Int. J.
746 Mass Spectrom., 286, 122-128, 2009.
747 Kanakidou, M., Seinfeld, J. H., Pandis, S. N., Barnes, I., Dentener, F. J., Facchini, M.
748 C., Van Dingenen, R., Ervens, B., Nenes, A., Nielsen, C. J., Swietlicki, E., Putaud, J.
749 P., Balkanski, Y., Fuzzi, S., Horth, J., Moortgat, G. K., Winterhalter, R., Myhre, C.
750 E. L., Tsigaridis, K., Vignati, E., Stephanou, E. G., and Wilson, J.: Organic aerosol
751 and global climate modelling: a review, Atmos. Chem. Phys., 5, 1053-1123,
752 10.5194/acp-5-1053-2005, 2005.
753 Kirchstetter, T. W., Harley, R. A., Kreisberg, N. M., Stolzenburg, M. R., and Hering, S.
754 V.: On-road measurement of fine particle and nitrogen oxide emissions from light-
755 and heavy-duty motor vehicles, Atmos. Environ., 33, 2955-2968,
756 http://dx.doi.org/10.1016/S1352-2310(99)00089-8, 1999.
757 Kroll, J. H., Chan, A. W. H., Ng, N. L., Flagan, R. C., and Seinfeld, J. H.: Reactions
758 of Semivolatile Organics and Their Effects on Secondary Organic Aerosol
759 Formation, Environ Sci Technol, 41, 3545-3550, 10.1021/es062059x, 2007.
760 Kroll, J. H., Smith, J. D., Worsnop, D. R., and Wilson, K. R.: Characterisation of
761 lightly oxidised organic aerosol formed from the photochemical aging of diesel
762 exhaust particles, Environmental Chemistry, 9, 211-220,

http://dx.doi.org/10.1071/EN11162, 2012.

Lindinger, W., Hansel, A., and Jordan, A.: On-line monitoring of volatile organic compounds at pptv levels by means of proton-transfer-reaction mass spectrometry (PTR-MS) medical applications, food control and environmental research, International Journal of Mass Spectrometry and Ion Processes, 173, 191-241, http://dx.doi.org/10.1016/S0168-1176(97)00281-4, 1998.

Liu, P. S. K., Deng, R., Smith, K. A., Williams, L. R., Jayne, J. T., Canagaratna, M. R., Moore, K., Onasch, T. B., Worsnop, D. R., and Deshler, T.: Transmission Efficiency of an Aerodynamic Focusing Lens System: Comparison of Model Calculations and Laboratory Measurements for the Aerodyne Aerosol Mass Spectrometer, Aerosol. Sci. Tech., 41, 721-733, 10.1080/02786820701422278, 2007.

Liu, T. Y., Wang, X. M., Wang, B. G., Ding, X., Deng, W., Lü, S. J., and Zhang, Y. L.: Emission factor of ammonia (NH_3) from on-road vehicles in China: tunnel tests in urban Guangzhou, Environ. Res. Lett., 9, 064027, 2014.

~~Lu, Z., Hao, J., Takekawa, H., Hu, L., and Li, J.: Effect of high concentrations of inorganic seed aerosols on secondary organic aerosol formation in the m-xylene/NO_x photooxidation system, Atmos. Environ., 43, 897-904, 2009.~~

McFiggans, G., Artaxo, P., Baltensperger, U., Coe, H., Facchini, M. C., Feingold, G., Fuzzi, S., Gysel, M., Laaksonen, A., Lohmann, U., Mentel, T. F., Murphy, D. M., O'Dowd, C. D., Snider, J. R., and Weingartner, E.: The effect of physical and chemical aerosol properties on warm cloud droplet activation, Atmos.

784 Chem. Phys., 6, 2593–2649, doi:10.5194/acp-6-2593-2006, 2006.
785 McMurry, P. H., and Grosjean, D.: Gas and aerosol wall losses in Teflon film smog
786 chambers, Environ. Sci. Technol., 19, 1176-1182, 10.1021/es00142a006, 1985.
787 Miracolo, M. A., Presto, A. A., Lambe, A. T., Hennigan, C. J., Donahue, N. M., Kroll,
788 J. H., Worsnop, D. R., and Robinson, A. L.: Photo-oxidation of low-volatility
789 organics found in motor vehicle emissions: Production and chemical evolution of
790 organic aerosol mass, Environ. Sci. Technol., 44, 1638-1643, 10.1021/es902635c,
791 2010.
792 National Bureau of Statistics of China: China Statistical Yearbook, Beijing: China
793 Statistics Press, 2013.
794 Nakao, S., Shrivastava, M., Nguyen, A., Jung, H., and Cocker, D.: Interpretation of
795 Secondary Organic Aerosol Formation from Diesel Exhaust Photooxidation in an
796 Environmental Chamber, Aerosol. Sci. Tech., 45, 964-972,
797 10.1080/02786826.2011.573510, 2011.
798 Ng, N. L., Kroll, J. H., Chan, A. W. H., Chhabra, P. S., Flagan, R. C., and Seinfeld, J.
799 H.: Secondary organic aerosol formation from m-xylene, toluene, and benzene,
800 Atmos. Chem. Phys., 7, 3909-3922, 10.5194/acp-7-3909-2007, 2007.
801 Ng, N. L., Canagaratna, M. R., Zhang, Q., Jimenez, J. L., Tian, J., Ulbrich, I. M.,
802 Kroll, J. H., Docherty, K. S., Chhabra, P. S., Bahreini, R., Murphy, S. M., Seinfeld,
803 J. H., Hildebrandt, L., Donahue, N. M., DeCarlo, P. F., Lanz, V. A., Prévôt, A. S. H.,
804 Dinar, E., Rudich, Y., and Worsnop, D. R.: Organic aerosol components observed in

805 Northern Hemispheric datasets from Aerosol Mass Spectrometry, Atmos. Chem.
806 Phys., 10, 4625-4641, 10.5194/acp-10-4625-2010, 2010.
807 Ng, N. L., Canagaratna, M. R., Jimenez, J. L., Chhabra, P. S., Seinfeld, J. H., and
808 Worsnop, D. R.: Changes in organic aerosol composition with aging inferred from
809 aerosol mass spectra, Atmos. Chem. Phys., 11, 6465-6474,
810 10.5194/acp-11-6465-2011, 2011.
811 Nordin, E. Z., Eriksson, A. C., Roldin, P., Nilsson, P. T., Carlsson, J. E., Kajos, M. K.,
812 Hellén, H., Wittbom, C., Rissler, J., Löndahl, J., Swietlicki, E., Svenningsson, B.,
813 Bohgard, M., Kulmala, M., Hallquist, M., and Pagels, J. H.: Secondary organic
814 aerosol formation from idling gasoline passenger vehicle emissions investigated in
815 a smog chamber, Atmos. Chem. Phys., 13, 6101-6116, 10.5194/acp-13-6101-2013,
816 2013.
817 Odum, J. R., Hoffmann, T., Bowman, F., Collins, D., Flagan, R. C., and Seinfeld, J. H.:
818 Gas/particle partitioning and secondary organic aerosol yields, Environ. Sci.
819 Technol., 30, 2580-2585, 10.1021/es950943+, 1996.
820 Odum, J. R., Jungkamp, T. P. W., Griffin, R. J., Forstner, H. J. L., Flagan, R. C., and
821 Seinfeld, J. H.: Aromatics, reformulated gasoline, and atmospheric organic aerosol
822 formation, Environ. Sci. Technol., 31, 1890-1897, 10.1021/es960535l, 1997.
823 Pankow, J. F.: An absorption-model of gas-particle partitioning of organic compounds
824 in the atmosphere, Atmos. Environ., 28, 185-188, 1994a.
825 Pankow, J. F.: An absorption-model of the gas aerosol partitioning involved in the

formation of secondary organic aerosol, Atmos. Environ., 28, 189-193, 1994b.

Pathak, R. K., Stanier, C. O., Donahue, N. M., and Pandis, S. N.: Ozonolysis of alpha-pinene at atmospherically relevant concentrations: Temperature dependence of aerosol mass fractions (yields), J Geophys Res-Atmos, 112, 10.1029/2006jd007436, 2007.

Platt, S. M., El Haddad, I., Zardini, A. A., Clairotte, M., Astorga, C., Wolf, R., Slowik, J. G., Temime-Roussel, B., Marchand, N., Ježek, I., Drinovec, L., Močnik, G., Möhler, O., Richter, R., Barmet, P., Bianchi, F., Baltensperger, U., and Prévôt, A. S. H.: Secondary organic aerosol formation from gasoline vehicle emissions in a new mobile environmental reaction chamber, Atmos. Chem. Phys., 13, 9141-9158, 10.5194/acp-13-9141-2013, 2013.

Presto, A. A., Gordon, T. D., and Robinson, A. L.: Primary to secondary organic aerosol: evolution of organic emissions from mobile combustion sources, Atmos. Chem. Phys., 14, 5015-5036, 10.5194/acp-14-5015-2014, 2014.

Robinson, A. L., Donahue, N. M., Shrivastava, M. K., Weitkamp, E. A., Sage, A. M., Grieshop, A. P., Lane, T. E., Pierce, J. R., and Pandis, S. N.: Rethinking Organic Aerosols: Semivolatile Emissions and Photochemical Aging, Science, 315, 1259-1262, 10.1126/science.1133061, 2007.

Samy, S., and Zielinska, B.: Secondary organic aerosol production from modern diesel engine emissions, Atmos. Chem. Phys., 10, 609-625, 10.5194/acp-10-609-2010, 2010.

847 Saxena, P., and Hildemann, L.: Water-soluble organics in atmospheric particles: A
848 critical review of the literature and application of thermodynamics to identify
849 candidate compounds, J. Atmos. Chem., 24, 57-109, 10.1007/BF00053823, 1996.
850 Schauer, J. J., Kleeman, M. J., Cass, G. R., and Simoneit, B. R. T.: Measurement of
851 emissions from air pollution sources. 5. C1−C32 organic compounds from
852 gasoline-powered motor vehicles, Environ. Sci. Technol., 36, 1169-1180,
853 10.1021/es0108077, 2002.
854 Shakya, K. M., and Griffin, R. J.: Secondary organic aerosol from photooxidation of
855 polycyclic aromatic hydrocarbons, Environ. Sci. Technol., 44, 8134-8139,
856 10.1021/es1019417, 2010.
857 Song, C., Na, K., Warren, B., Malloy, Q., and Cocker, D. R.: Impact of Propene on
858 Secondary Organic Aerosol Formation from m-Xylene, Environ Sci Technol, 41,
859 6990-6995, 10.1021/es062279a, 2007.
860 Tkacik, D. S., Presto, A. A., Donahue, N. M., and Robinson, A. L.: Secondary organic
861 aerosol formation from intermediate-volatility organic compounds: cyclic, linear,
862 and branched alkanes, Environ. Sci. Technol., 46, 8773-8781, 10.1021/es301112c,
863 2012.
864 Tkacik, D. S., Lambe, A. T., Jathar, S., Li, X., Presto, A. A., Zhao, Y. L., Blake, D.,
865 Meinardi, S., Jayne, J. T., Croteau, P. L., and Robinson, A. L.: Secondary Organic
866 Aerosol Formation from in-Use Motor Vehicle Emissions Using a Potential Aerosol
867 Mass Reactor, Environ Sci Technol, 48, 11235-11242, 10.1021/es502239v, 2014.

868 Tong, H. Y., Hung, W. T., and Cheung, C. S.: On-road motor vehicle emissions and
869 fuel consumption in urban driving conditions, Journal of the Air & Waste
870 Management Association, 50, 543-554, 2000.
871 Volkamer, R., Jimenez, J. L., San Martini, F., Dzepina, K., Zhang, Q., Salcedo, D.,
872 Molina, L. T., Worsnop, D. R., and Molina, M. J.: Secondary organic aerosol
873 formation from anthropogenic air pollution: Rapid and higher than expected,
874 Geophys. Res. Lett., 33, L17811, 10.1029/2006gl026899, 2006.
875 Wagner, D. V., An, F., and Wang, C.: Structure and impacts of fuel economy standards
876 for passenger cars in China, Energy. Policy., 37, 3803-3811,
877 doi:10.1016/j.enpol.2009.07.009, 2009.
878 Wang, J., Jin, L., Gao, J., Shi, J., Zhao, Y., Liu, S., Jin, T., Bai, Z., and Wu, C.-Y.:
879 Investigation of speciated VOC in gasoline vehicular exhaust under ECE and
880 EUDC test cycles, Sci. Total Environ., 445–446, 110-116,
881 http://dx.doi.org/10.1016/j.scitotenv.2012.12.044, 2013.
882 Wang, X. H., Bi, X. H., Sheng, G. Y., and Fu, J. M.: Chemical composition and
883 sources of PM_{10} and $PM_{2.5}$ aerosols in Guangzhou, China, Environ. Monit. Assess.,
884 119, 425-439, DOI 10.1007/s10661-005-9034-3, 2006.
885 Wang, X. M., and Wu. T.: Release of isoprene and monoterpenes during the aerobic
886 decomposition of orange wastes from laboratory incubation experiments, Environ.
887 Sci. Technol., 42, 3265-3270, 2008.
888 Wang, X., Liu, T., Bernard, F., Ding, X., Wen, S., Zhang, Y., Zhang, Z., He, Q., Lü, S.,

889 Chen, J., Saunders, S., and Yu, J.: Design and characterization of a smog chamber
890 for studying gas-phase chemical mechanisms and aerosol formation, Atmos. Meas.
891 Tech., 7, 301-313, 10.5194/amt-7-301-2014, 2014.
892 Wehner, B., Wiedensohler, A., Tuch, T. M., Wu, Z. J., Hu, M., Slanina, J., and Kiang,
893 C. S.: Variability of the aerosol number size distribution in Beijing, China: New
894 particle formation, dust storms, and high continental background, Geophys. Res.
895 Lett., 31, L22108, 10.1029/2004GL021596, 2004.
896 Weitkamp, E. A., Sage, A. M., Pierce, J. R., Donahue, N. M., and Robinson, A. L.:
897 Organic aerosol formation from photochemical oxidation of diesel exhaust in a
898 smog chamber, Environ. Sci. Technol., 41, 6969-6975, 10.1021/es070193r, 2007.
899 Yang, H., Yu, J. Z., Ho, S. S. H., Xu, J. H., Wu, W. S., Wan, C. H., Wang, X. D., Wang,
900 X. R., and Wang, L. S.: The chemical composition of inorganic and carbonaceous
901 materials in $PM_{2.5}$ in Nanjing, China, Atmos. Environ., 39, 3735-3749, DOI
902 10.1016/j.atmosenv.2005.03.010, 2005.
903 Yi, Z., Wang, X., Sheng, G., Zhang, D., Zhou, G., and Fu, J.: Soil uptake of carbonyl
904 sulfide in subtropical forests with different successional stages in south China, J.
905 Geophys. Res., 112, D08302, 10.1029/2006JD008048, 2007.
906 Zhang, Q., Worsnop, D. R., Canagaratna, M. R., and Jimenez, J. L.: Hydrocarbon-like
907 and oxygenated organic aerosols in Pittsburgh: insights into sources and processes
908 of organic aerosols, Atmos. Chem. Phys., 5, 3289-3311, 10.5194/acp-5-3289-2005,
909 2005.

910 Zhang, Q., Jimenez, J. L., Canagaratna, M. R., Allan, J. D., Coe, H., Ulbrich, I.,
911 Alfarra, M. R., Takami, A., Middlebrook, A. M., Sun, Y. L., Dzepina, K., Dunlea,
912 E., Docherty, K., DeCarlo, P. F., Salcedo, D., Onasch, T., Jayne, J. T., Miyoshi, T.,
913 Shimono, A., Hatakeyama, S., Takegawa, N., Kondo, Y., Schneider, J., Drewnick,
914 F., Borrmann, S., Weimer, S., Demerjian, K., Williams, P., Bower, K., Bahreini, R.,
915 Cottrell, L., Griffin, R. J., Rautiainen, J., Sun, J. Y., Zhang, Y. M., and Worsnop, D.
916 R.: Ubiquity and dominance of oxygenated species in organic aerosols in
917 anthropogenically-influenced Northern Hemisphere midlatitudes, Geophys. Res.
918 Lett., 34, L13801, 10.1029/2007gl029979, 2007.
919 Zhang, Q., He, K., and Huo, H.: Policy: Cleaning China's air, Nature, 484, 161-162,
920 2012.
921 Zhang, X., Cappa, C. D., Jathar, S. H., McVay, R. C., Ensberg, J. J., Kleeman, M. J.,
922 and Seinfeld, J. H.: Influence of vapor wall loss in laboratory chambers on yields of
923 secondary organic aerosol, Proceedings of the National Academy of Sciences,
924 10.1073/pnas.1404727111, 2014.
925 Zhang, X., Schwantes, R. H., McVay, R. C., Lignell, H., Coggon, M. M., Flagan, R.
926 C., and Seinfeld, J. H.: Vapor wall deposition in Teflon chambers, Atmos. Chem.
927 Phys., 15, 4197-4214, 10.5194/acp-15-4197-2015, 2015.
928 Zhang, Y. L., Guo, H., Wang, X. M., Simpson, I. J., Barletta, B., Blake, D. R.,
929 Meinardi, S., Rowland, F. S., Cheng, H. R., Saunders, S. M., and Lam, S. H. M.:
930 Emission patterns and spatiotemporal variations of halocarbons in the Pearl River

931 Delta region, southern China. J. Geophys. Res., 115, D15309,
932 doi:10.1029/2009JD013726, 2010
933 Zhang, Y., Wang, X., Blake, D. R., Li, L., Zhang, Z., Wang, S., Guo, H., Lee, F. S. C.,
934 Gao, B., Chan, L., Wu, D., and Rowland, F. S.: Aromatic hydrocarbons as ozone
935 precursors before and after outbreak of the 2008 financial crisis in the Pearl River
936 Delta region, south China, J. Geophys. Res., 117, D15306, 10.1029/2011JD017356,
937 2012.
938 Zhang, Y., Wang, X., Zhang, Z., Lü, S., Shao, M., Lee, F. S. C., and Yu, J.: Species
939 profiles and normalized reactivity of volatile organic compounds from gasoline
940 evaporation in China, Atmos. Environ., 79, 110-118,
941 http://dx.doi.org/10.1016/j.atmosenv.2013.06.029, 2013.
942 Zhang, Y. L., Wang, X. M., Li, G. H., Yang, W. Q., Huang, Z. H., Zhang, Z., Huang, X.
943 Y., Deng, W., Liu, T. Y., Huang, Z. Z., and Zhang, Z. Y.: Emission factors of fine
944 particles, carbonaceous aerosols and traces gases from road vehicles: recent tests in
945 an urban tunnel in the Pearl River Delta, China, Atmos. Environ., in review, 2015.
946

947 **Table 1.** Detailed information of the two light-duty gasoline vehicles.

ID	Emission standard class	Vehicle	Model year	Mileage (km)	Displacement (cm^3)	Power (kW)	Weight (kg)
Ⅰ	Euro4	Golf	2011	25000	1598	77	1295
II	Euro1	Accord	2002	237984	2298	110	1423

948

949

Table 2. Initial conditions for the light-duty gasoline vehicle photooxidation experiments.

Experiment #	Vehicle ID	T (℃)[a]	RH (%)[a]	VOC/ NO_x	~~NMHCs~~ VOCs (ppbv)[b]	NO (ppbv)	NO_2 (ppbv)
1	Ⅰ	25.8±0.7	52.0±1.8	10.2	1368	115.1	18.4
2	II	24.1±0.6	57.0±2.0	6.0	2583	431.0	0.6
3	Ⅰ	25.0±0.8	52.9±2.0	9.3	2896	300.6	9.5
4	Ⅰ	24.2±0.8	52.5±2.7	2.0	1885	794.1	161.9
5	II	25.0±0.3	52.6±1.3	7.2	1507	210.4	0.7

[a]: Stated uncertainties (1 σ) are from scatter in temperature and relative humidity, respectively.

[b]: C2-C3 and C4-C12 hydrocarbons were measured by GC-FID and GC-MSD, respectively.

Table 43. Summary of the results for the light-duty gasoline vehicle photooxidation experiments.

Exp #	Vehicle ID	OH ($\times 10^6$ molecules cm^{-3})	POA ($\mu g\ m^{-3}$)	SOA ($\mu g\ m^{-3}$)	SOA/POA	Effective yield
1	I	1.23	1.1	51.1	46	0.103
2	II	0.73	0.2	17.6	88	0.038
3	I	0.88	0.3	77.6	259	0.119
4	I	1.20	1.0	125.4	125	0.172
5	II	0.79	0.3	4.0	12	0.028

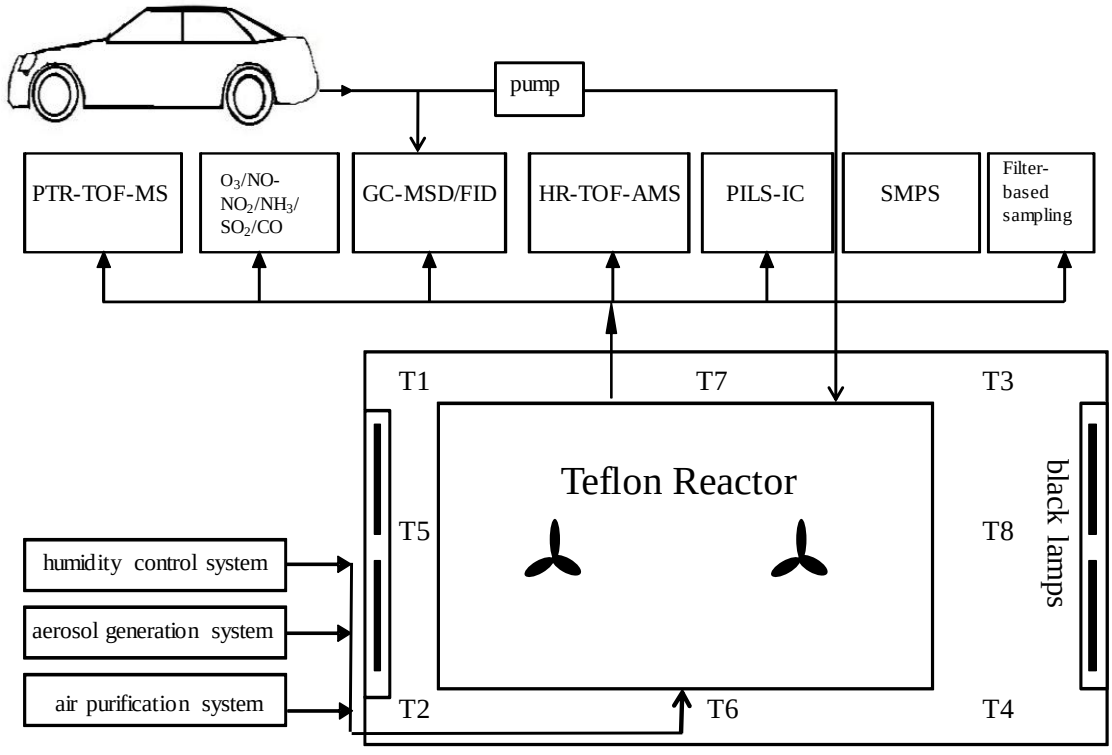

959

960 **Fig. 1**. Schematic of the GIG-CAS smog chamber facility and vehicle exhaust

961 injection system.

962

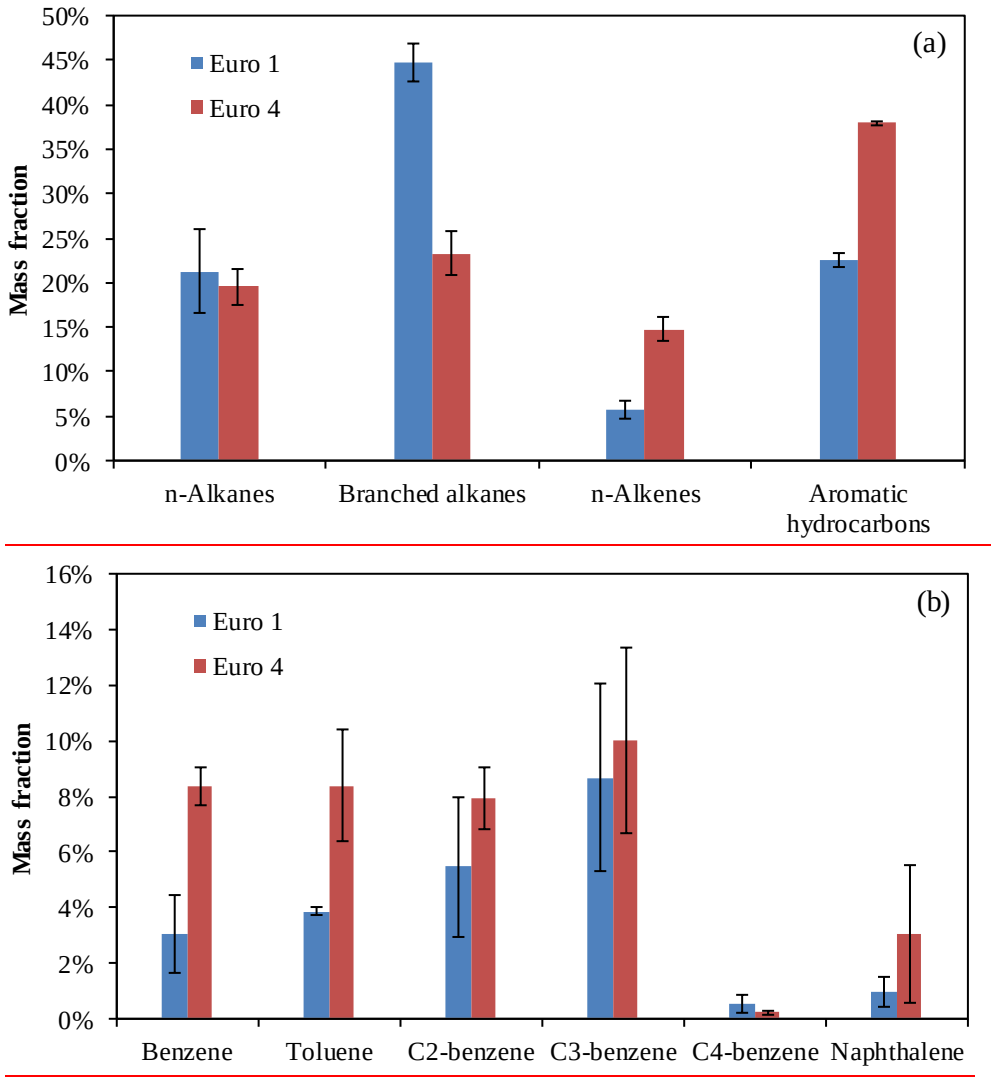

Fig. 42. Composition of **(a)** VOCs and **(b)** aromatics of gasoline vehicle exhausts from Euro 1 and Euro 4 private cars, presented as weight percentage of speciated VOCs. C2-C3 and C4-C12 hydrocarbons were measured by GC-FID and GC-MSD, respectively. The error bars (1 σ) represent variability from measurements for each vehicle.

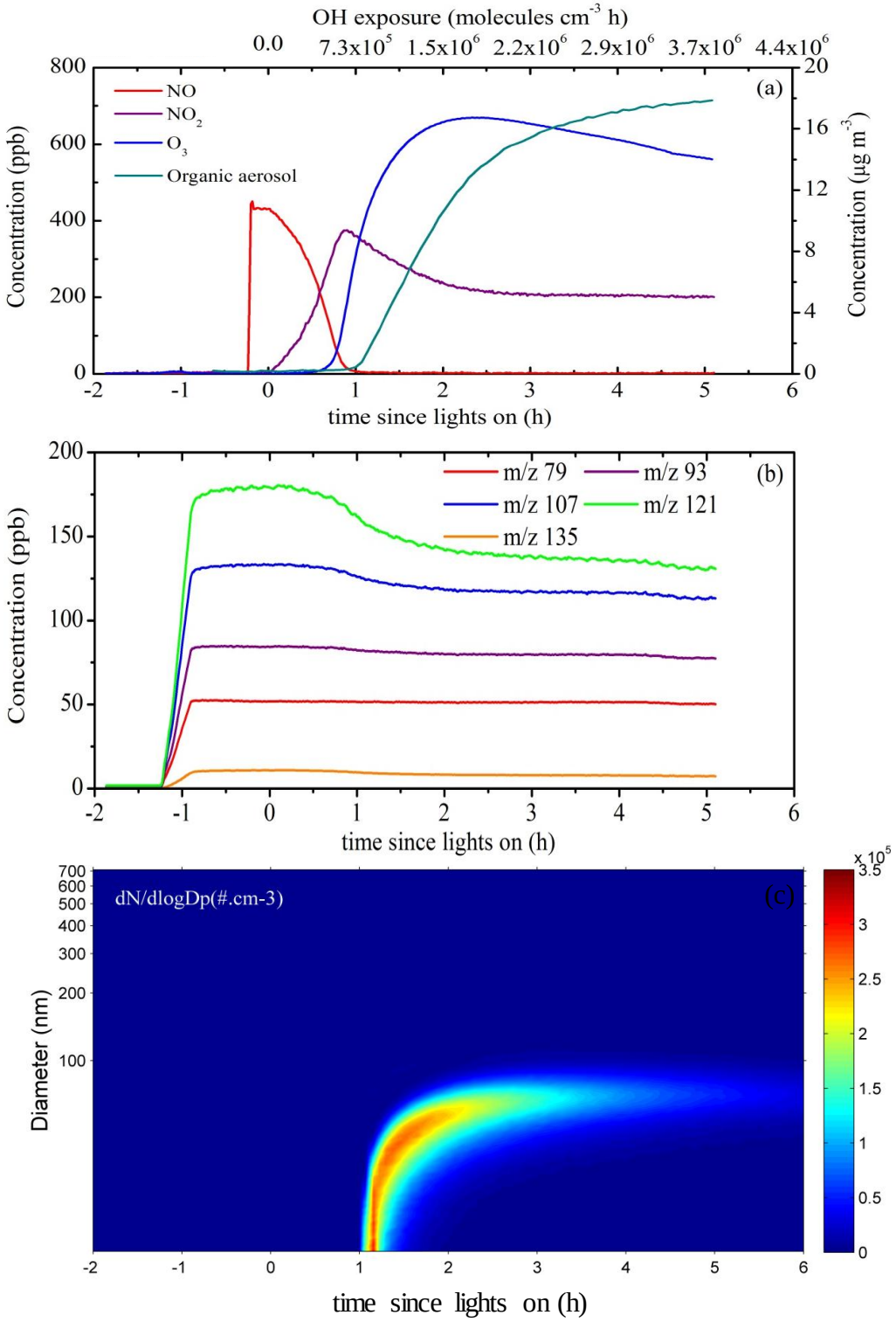

971

972 **Fig. ~~5~~3**. Concentration–time plots of gas–phase and particle–phase species and
973 particle number concentration distribution as a function of time during a typical smog
974 chamber experiment (experiment 2): **(a)** NO, NO_2, O_3 (left *y* axis) and organic aerosol
975 (right *y* axis); **(b)** gas-phase light aromatics (measured by PTR-TOF-MS) (benzene

characterized by m/z 79; toluene characterized by m/z 93; C_2–benzene characterized by m/z 107; C_3–benzene characterized by m/z 121; C_4-benzene characterized by m/z 135); **(c)** particle size-number concentration distributions as a function of time. The vehicle exhaust was introduced into the reactor between -1.3 h and -0.85 h; the primary emissions were characterized from -0.85 h to 0 h; at time = 0 h, the black lamps were turned on.

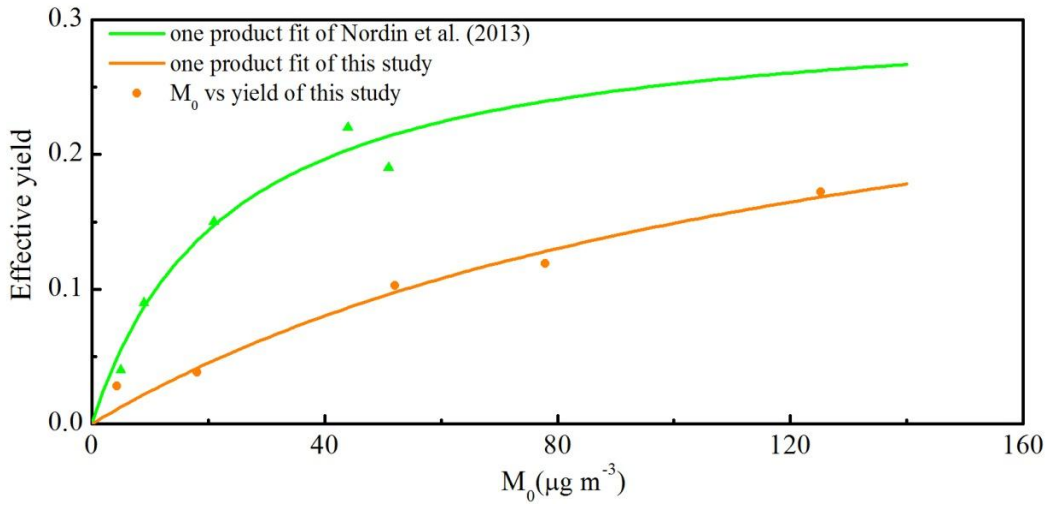

Fig. ~~6~~4. Comparison of yield data obtained for the gasoline experiments in this study with that of Nordin et al. (2013). The green line is the best fit one-product model (α_1 = 0.311, $K_{om,1}$ = 0.043) for the data set of Nordin et al. (2013). The orange line is the best one-product fit to the effective SOA yield in this study (α_1 = 0.350, $K_{om,1}$ = 0.007). Organic precursors in the calculation of effective yields included benzene, toluene, C2–benzene, C3–benzene, C4-benzene and naphthalene.

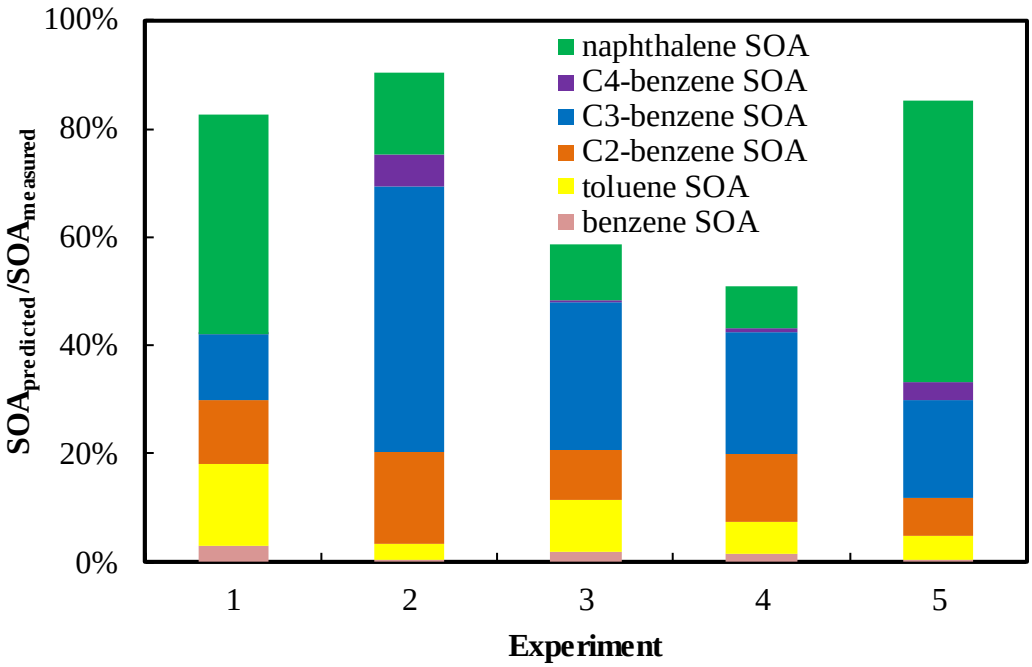

Fig. ~~7~~5. Contributions of the predicted benzene SOA, toluene SOA, C2–benzene SOA, C3–benzene SOA, C4–benzene SOA and naphthalene SOA to the total formed SOA in all experiments.

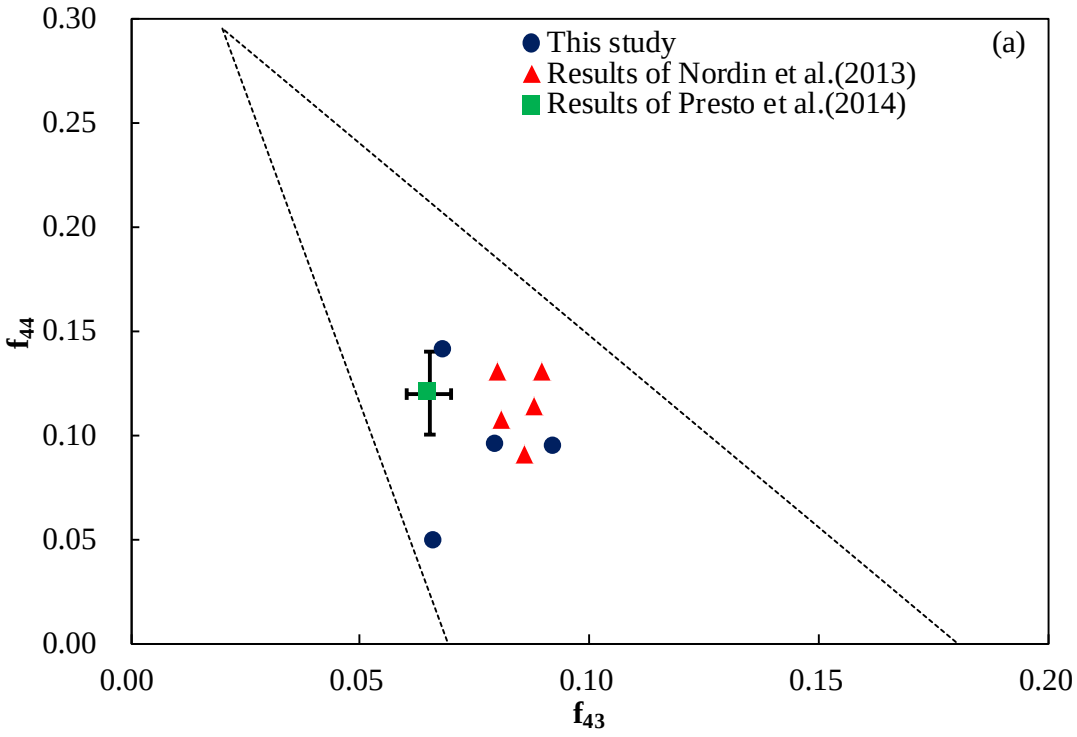

997

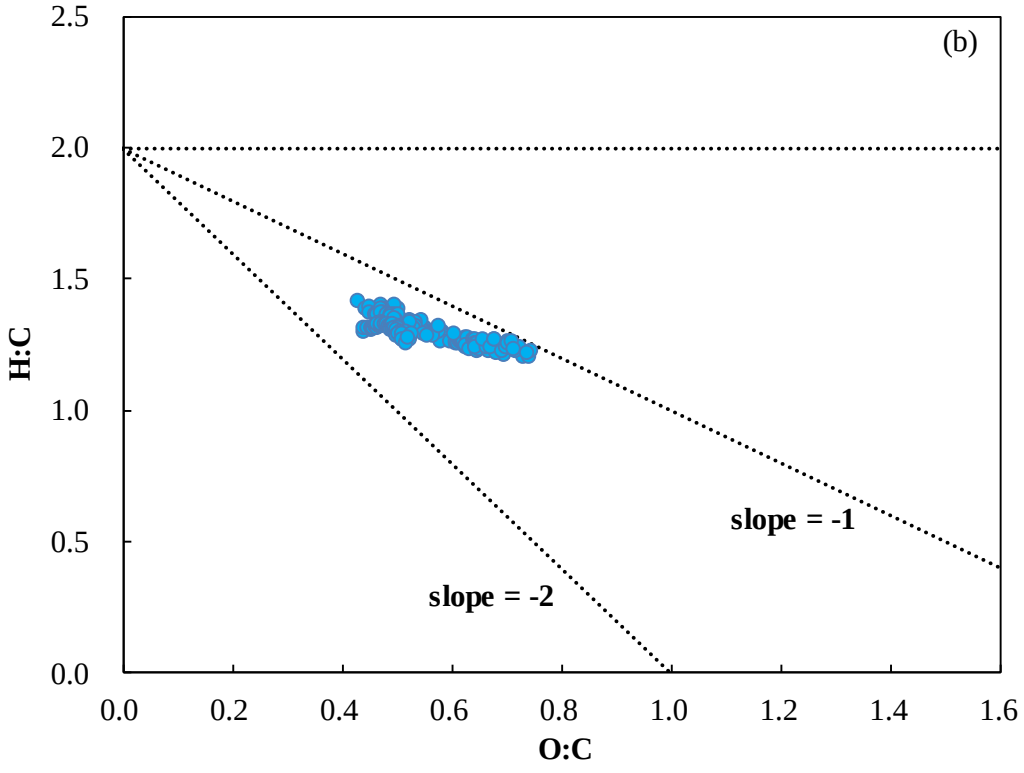

998

999 **Fig. ~~8~~6. (a)** The fractions of total organic signal at m/z 43 (f_{43}) vs. m/z (f_{44}) at the end
1000 of each experiment together with the triangle plot of Ng et al. (2010). The solid square
1001 and triangles represent the results of Presto et al. (2014) and Nordin et al. (2013),
1002 respectively. The dotted lines define the space where ambient OOA components fall.

The ranges of f_{44} observed for SV-OOA and LV-OOA components are 0.03–0.11 and 0.13–0.21**,** respectively. **(b)** Van Krevelen diagram of SOA from light-duty gasoline vehicle exhaust. Dotted lines are to show slopes of 0, -1 and -2. AMS data of the experiment 5 were unavailable.